



저작자표시-비영리-변경금지 2.0 대한민국

이용자는 아래의 조건을 따르는 경우에 한하여 자유롭게

- 이 저작물을 복제, 배포, 전송, 전시, 공연 및 방송할 수 있습니다.

다음과 같은 조건을 따라야 합니다:



저작자표시. 귀하는 원 저작자를 표시하여야 합니다.



비영리. 귀하는 이 저작물을 영리 목적으로 이용할 수 없습니다.



변경금지. 귀하는 이 저작물을 개작, 변형 또는 가공할 수 없습니다.

- 귀하는, 이 저작물의 재이용이나 배포의 경우, 이 저작물에 적용된 이용허락조건을 명확하게 나타내어야 합니다.
- 저작권자로부터 별도의 허가를 받으면 이러한 조건들은 적용되지 않습니다.

저작권법에 따른 이용자의 권리와 책임은 위의 내용에 의하여 영향을 받지 않습니다.

이것은 [이용허락규약\(Legal Code\)](#)을 이해하기 쉽게 요약한 것입니다.

[Disclaimer](#)



Allicin induces brown-like adipocytes formation via KLF15 signal cascade

Chung Gi LEE

**The Graduate School
Sungkyunkwan University
Department of Pharmacy**

Allicin induces brown-like adipocytes formation via KLF15 signal cascade

Chung Gi LEE

**The Graduate School
Sungkyunkwan University
Department of Pharmacy**

Allicin induces brown-like adipocytes formation via KLF15 signal cascade

Chung Gi LEE

**A Dissertation Submitted to the Department of Pharmacy
and the Graduate School of Sungkyunkwan University
in partial fulfillment of the requirements
for the degree of Ph.D. in Pharmacy**

April 2018

Approved by

Suhkneung Pyo

Major Advisor

This certifies that the dissertation
of Chung Gi LEE is approved.

Thesis Supervisor

Thesis Committee Chairman

Thesis Committee Member

Thesis Committee Member

Thesis Committee Member

The Graduate School
Sungkyunkwan University
June 2018

CONTENTS

List of Tables -----	vii
List of Figures -----	viii
Abstract -----	x

I. INTRODUCTION

1. Obesity -----	1
-------------------------	---

2. Brown and white adipocytes -----	3
--	---

2.1 Subcutaneous WAT and visceral WAT -----	3
2.2 Adipocyte turnover -----	5

3. Adipocyte dysfunction and inflammation -----	6
--	---

3.1 ER stress in adipocytes -----	6
3.2 Mitochondrial dysfunction and inflammation in adipocytes -----	7

4. Therapeutic approaches for obesity -----	9
--	---

5. UCP1 in brown adipocytes	10
5.1 Uncoupling protein 1	10
5.2 Regulatory mechanism of UCP1 expression	12
6. White adipocyte browning	13
7. Allicin: an active compound in garlic	15
7.1 Therapeutic properties of garlic	15
7.2 Antioxidant and anti-inflammatory effects of allicin	16
8. KLF15	18
9. Aim of Study	19

II. MATERIALS AND METHODS

1. Materials	21
1.1 Chemicals	21
1.2 Instruments	24
2. Methods	25
2.1 Reagents and purification of allicin	25
2.2 Cell culture and differentiation	26
2.3 Animals	27
2.4 Isolation of total RNA and quantitative real-time PCR	28
2.5 Determination of lipid accumulation by Oil Red O staining	29
2.6 Mitotracker staining and confocal laser microscopy	29
2.7 Western blot analysis	30
2.8 siRNAs	31
2.9 Chromatin immunoprecipitation assay	31
2.10 Immunohistochemistry	32
2.11 Statistical analysis	33

III. RESULTS

1. Effect of allicin on expression of brown adipocyte-selective genes in white adipocytes -----	34
2. Effect of allicin on accumulation of mitochondria in white adipocytes -- -----	35
3. Effect of allicin on KLF15 expression in white adipocytes -----	38
4. Effect of KLF15 on allicin-induced UCP1 expression in white adipocytes -----	39
5. Effect of allicin on phosphorylation of MAPK in white adipocytes -----	40
6. Effect of ERK signaling on allicin-induced browning of white adipocytes -----	41

7. Effect of allicin on association between KLF15 and UCP1 promoter region	44
8. Effect of allicin on body weight in mice	45
9. Effect of allicin on adipocyte browning of iWAT in mice	47
10. Effect of allicin on lipid oxidation and energy expenditure in mice	51
11. Effect of allicin on lipid metabolism in mice	52
IV. DISCUSSION	54
.	

V. REFERENCES ----- 59

ABSTRACT (Korean) ----- 74

List of Tables

Table 1. Primer sequences and real-time PCR conditions ----- 29

List of Figures

Figure 1. Relationship between energy balance and energy expenditure -----	2
Figure 2. Key factors involved in regulating energy balance -----	2
Figure 3. Types of adipocytes -----	3
Figure 4. Biological effect of white adipose tissue on other tissues in the body -----	4
Figure 5. Subcutaneous obesity and visceral obesity -----	5
Figure 6. Healthy white adipose tissue expansion versus unhealthy pathological expansion in obesity -----	7
Figure 7. Molecular pathways of inflammatory responses with insulin action in adipocytes - -----	9
Figure 8. Therapeutic strategies for obesity by BMI category -----	10
Figure 9. UCP1-mediated uncoupling of respiration from ATP synthesis -----	11
Figure 10. UCP1-mediated of thermogenesis in brown adipocytes -----	13
Figure 11. Cold-induced differentiation of brown-like/beige adipocytes -----	15
Figure 12. Biosynthesis of allicin -----	17
Figure 13. Regulatory mechanism of KLF15 on switching between lipogenesis and gluconeogenesis during fasting -----	19
Figure 14. Effect of allicin on expression of brown adipocyte-selective genes in white adipocytes -----	34
Figure 15. Effect of allicin on the accumulation of mitochondria in white adipocytes -----	36
Figure 16. Effect of allicin on KLF15 expression in white adipocytes -----	38
Figure 17. Effect of KLF15 on allicin-induced UCP1 expression in white adipocytes -----	39
Figure 18. Effect of allicin on activation of MAPK in white adipocytes -----	40

Figure 19. Effect of ERK on allicin-induced browning of white adipocytes -----	42
Figure 20. Effect of allicin on the association between KLF15 and UCP1 promoter region - -----	45
Figure 21. Effect of allicin on body weight in mice -----	46
Figure 22. Effect of allicin on adipocyte browning of iWAT in mice -----	48
Figure 23. Effect of allicin on lipid oxidation and energy expenditure in mice -----	51
Figure 24. Effect of allicin on lipid metabolism in mice -----	53

Abstract

Allicin induces brown-like adipocytes formation via KLF15 signal cascade

Obesity is defined as a condition of excess accumulation of white adipose tissue, accompanied by low grade inflammation. It has been reported that the chronic low-grade inflammation is associated with other metabolic syndromes such as insulin resistance, type 2 diabetes mellitus, and some types of cancer. Lifestyle interventions, pharmacotherapy, and bariatric surgery are considered as therapeutic strategy for obesity. However, these therapeutic options have limitation, like side effects. Thus, effective therapeutic options for obesity are urgently needed. In recent years, growing body of evidence indicates that brown-like adipocyte is generated in response to stimulation such as low temperatures and some hormones and enzymes. Because of its ability to increase energy expenditure and appear within white adipocytes, to promote the formation of brown-like adipocyte shows important therapeutic potential for obesity. However, whether diet-derived factors directly induce browning of white adipocytes is unknown. Thus, the effect of allicin, one of major components in garlic, on brown-like adipocyte formation in differentiated white adipocytes was investigated. Moreover,

the effect of allicin on lipid metabolism and prevention of obesity in animal models was investigated. In the present study, allicin significantly increased the mRNA and/or protein expression of brown adipocyte markers, including uncoupling protein 1 (UCP1) in the differentiated mouse embryonic fibroblast cell line 3T3-L1 and differentiated iWAT stromal vascular cells (SVC), suggesting that allicin induced brown-like adipocyte formation in vitro. Concomitantly, allicin markedly enhanced the protein expression of KLF15 and its interaction with the UCP1 promoter region. Such changes were not observed in KLF15-deficient cells, suggesting the critical role of KLF15 in allicin action. In allicin-administrated mice, allicin prevented the the body weight gain. Additionally, allicin promoted brown-like adipogenesis in vivo along with the appearance of multilocular adipocytes, increased UCP1 expression, and increased lipid oxidation. In summary, the present data suggest that allicin prevents obesity by enhancing the expression of brown adipocyte-specific genes, including UCP1, through the KLF15 signal cascade. Because obesity is a major risk factor for insulin resistance and type 2 diabetes, allicin may also be used to treat obesity-related metabolic diseases.

Key words: Allicin, Obesity, Brown-like adipocyte, KLF15, UCP1

I. INTRODUCTION

1. Obesity

Obesity is defined as excessive body weight relative to height along with increased accumulation of adipose tissue [1]. According to the World Health Organization, more than 1.9 billion adults were estimated to be overweight or obese globally in 2016, of which 650 million adults were obese. A total of 11% of adult men and 15% of adult women were obese in 2016, suggesting that the female sex may be associated with a higher risk of obesity [2]. According to the first law of thermodynamics, increased fat accumulation results from an imbalance between the consumption of high-energy-yielding foods and energy expenditure [1]. However, the etiology of obesity is complex [3]. Because socioeconomic status, environment, lifestyle, and genetic influences affect food intake, thermogenesis, and utilization and storage of fatty acids, these factors should be considered to understand obesity [4].

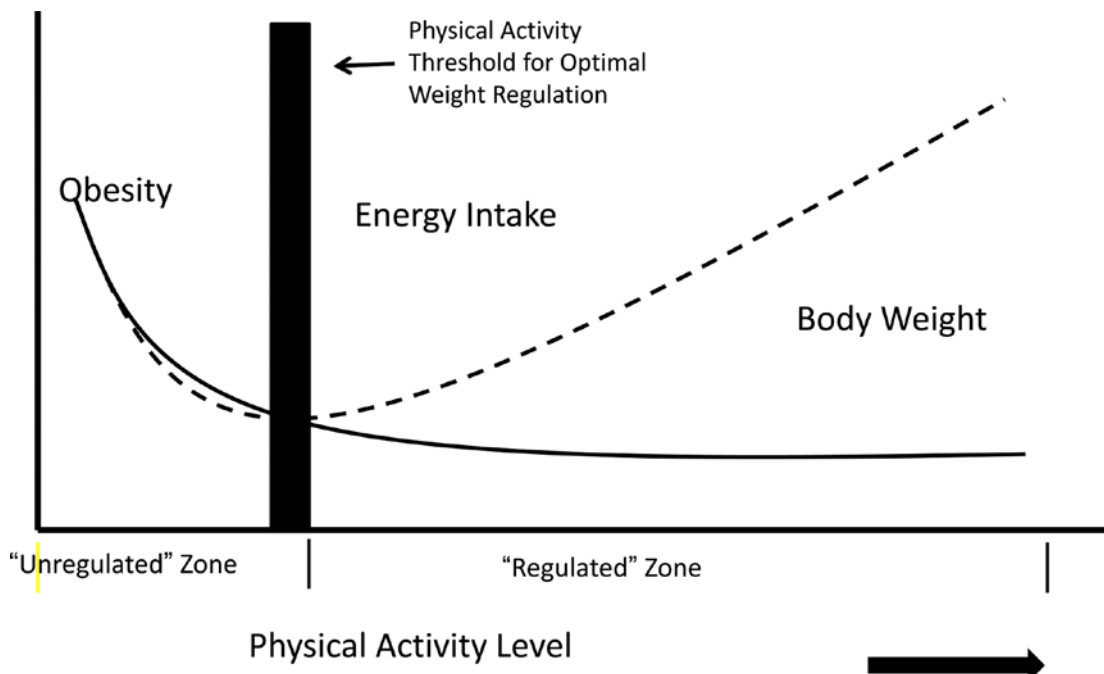


Figure 1. Relationship between energy balance and energy expenditure [5]

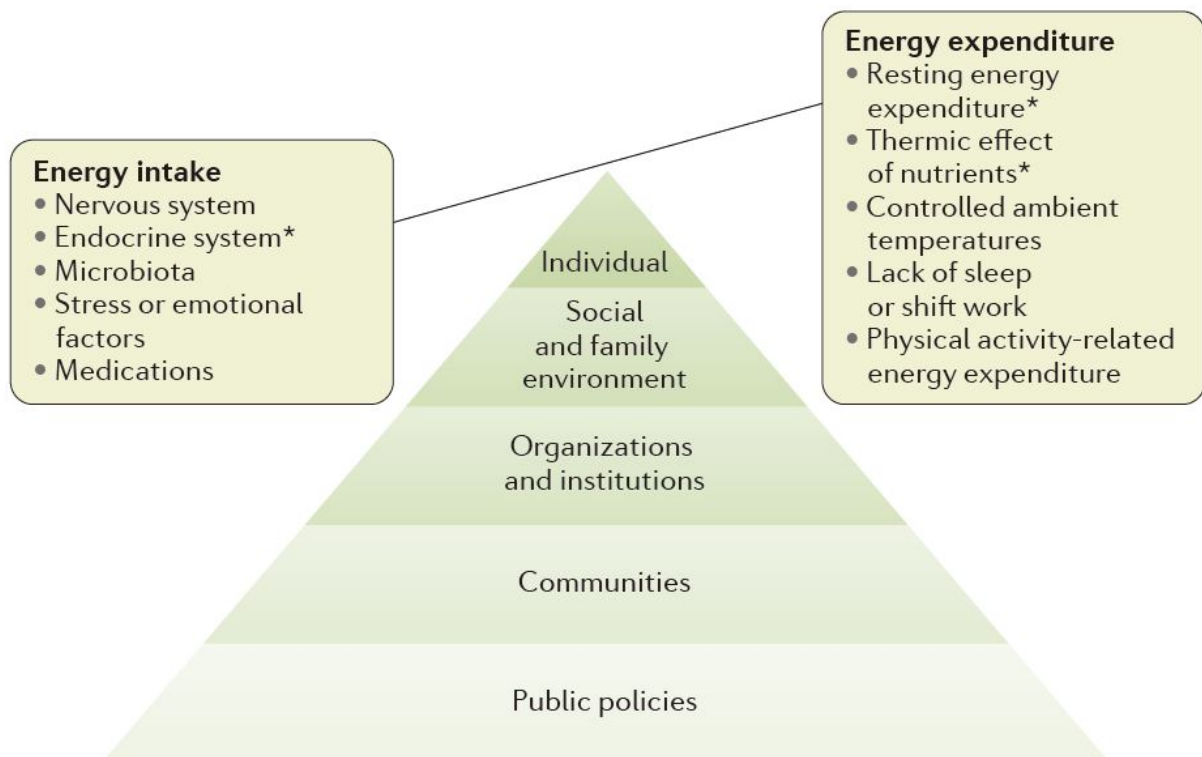


Figure 2. Key factors involved in regulating energy balance [1]

2. Brown and white adipocytes

White adipose tissue and brown adipose tissue, the two major types of adipose tissues, play critical roles in regulating systemic energy balance. Adipocytes in brown adipose tissue increase energy expenditure through thermogenesis to maintain body temperature [3]. Brown adipose tissue is abundant in newborn infants, but decreases with age. The adipose tissue can be found in the interscapular and supraclavicular region, as well as around the kidneys, heart, aorta, pancreas, and trachea [6].

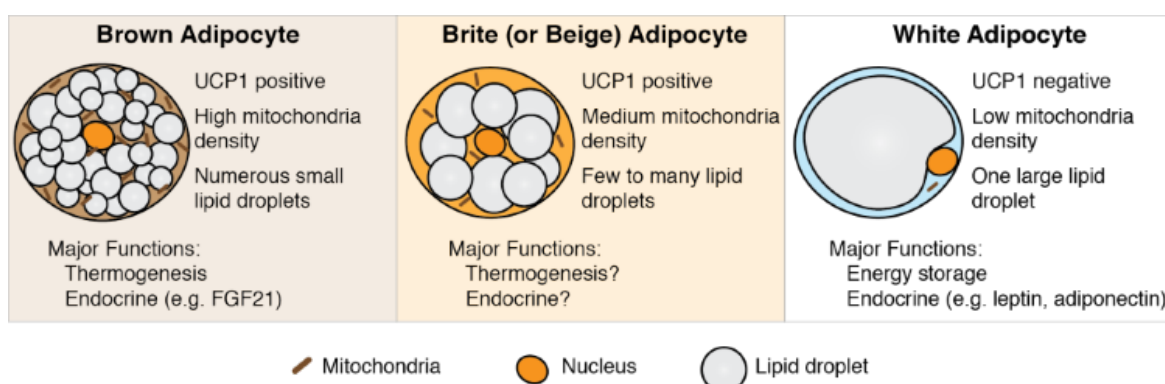


Figure 3. Types of adipocytes [7]

2.1. Subcutaneous WAT and visceral WAT

Originally, WAT was regarded as a repository for excess calories in the fed state. Free fatty acids are released in the fasted state from WAT to fuel the energy demands of the organism [8]. However, it has been revealed that WAT is a complex endocrine organ that regulates systemic energy homeostasis [9, 10]. In addition to secreting various adipocyte-derived factors

known as adipokines to regulate energy balance, WAT plays key roles in inflammation, organ protection, and thermoregulation. Based on its location, WAT can be classified into visceral adipose tissue, including intra-abdominal, perirenal, and pericardial adipose tissue, and subcutaneous adipose tissue [11]. A previous study showed that subcutaneous WAT has protective effects on energy homeostasis, whereas increased intra-abdominal visceral WAT is associated with metabolic disease risk [12].

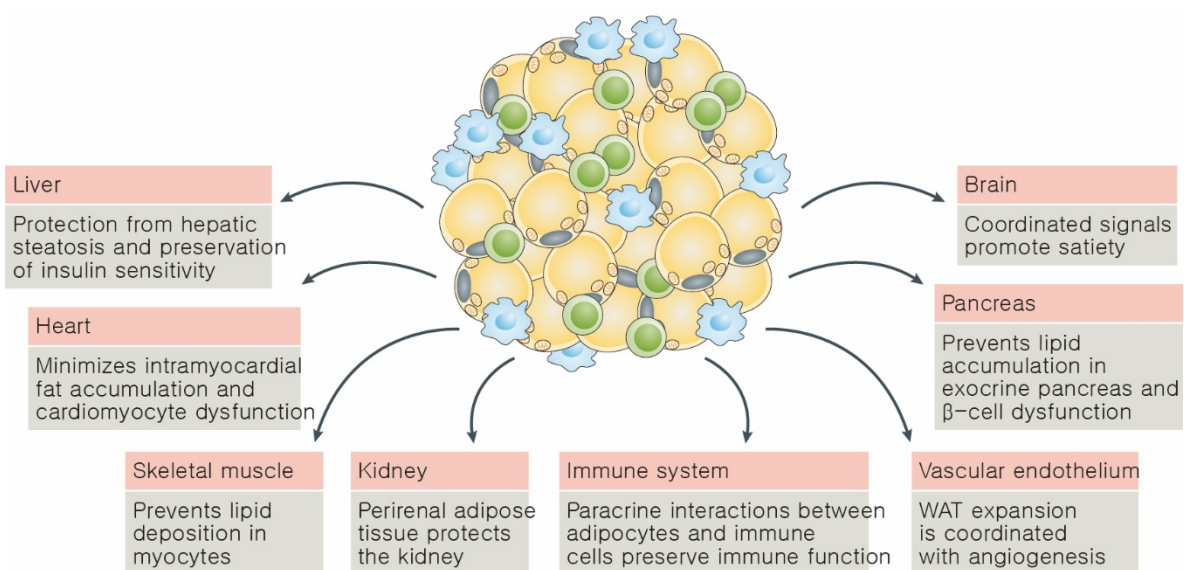


Figure 4. Biological effect of white adipose tissue on other tissues in the body [8]

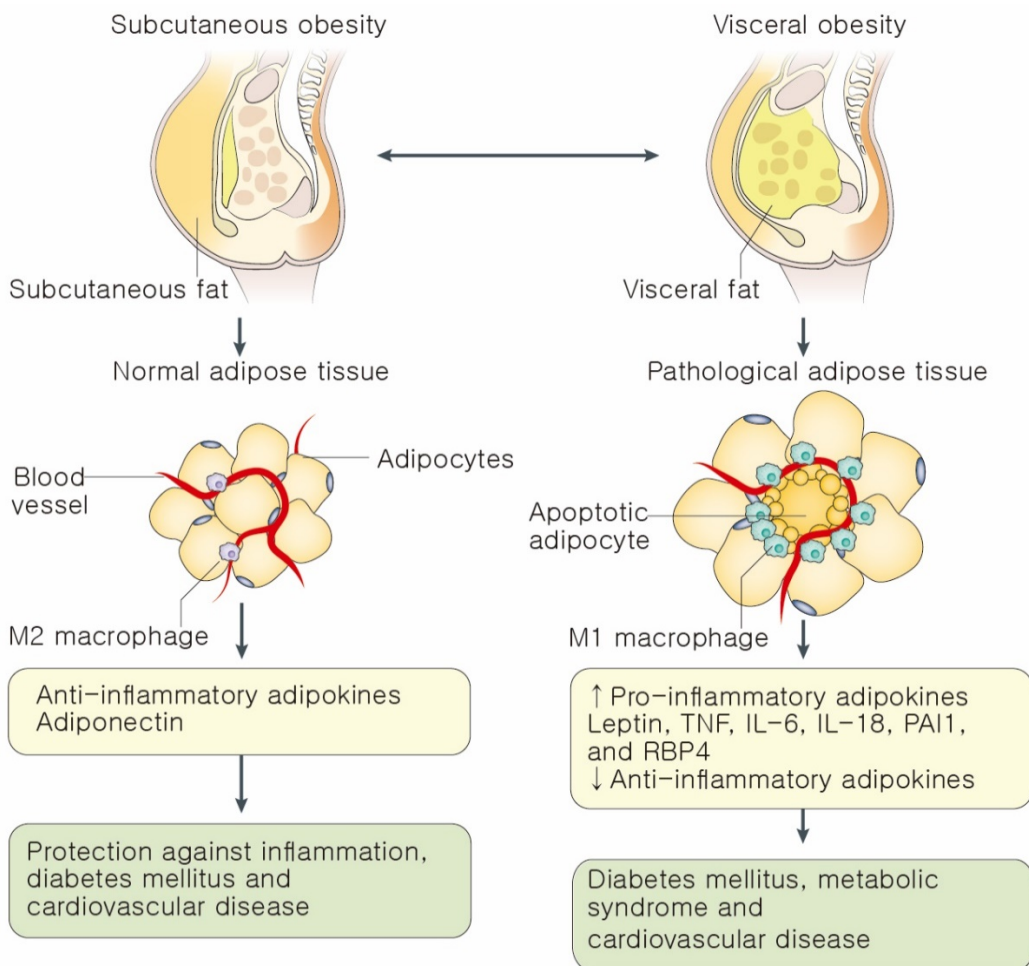


Figure 5. Subcutaneous obesity and visceral obesity [1]

2.2. Adipocyte turnover

Adipocyte turnover is currently thought to be sustained throughout adult life by maintaining the balance between adipogenesis and apoptosis. Total adipocyte numbers are strictly regulated during adulthood, even in obesity [8]. The total number of adipocytes is determined during childhood and adolescence. The mean life span of an adipocyte in adult humans is less than 10 years, with less than 10% of human subcutaneous WAT renewed each year [13].

3. Adipocyte dysfunction and inflammation

3.1. ER stress in adipocytes

WAT alters its size, function, inflammation state, and body distribution in response to nutrition status by remodeling, regulated by cellular signal cascades. At the cellular level, the size and number, oxidative stress level, adipokine secretory profile, and composition of infiltrated immune cells of white adipocytes are altered [14]. Particularly, excessive lipid accumulation appears to cause dysfunction of the endoplasmic reticulum (ER) and mitochondria in adipocytes. Because the ER regulates protein synthesis, lipid-droplet formation, and cholesterol synthesis in response to nutritional stimuli, excessive ER stress results in dysfunction of the ER in the states of energy imbalance and obesity [15]. Additionally, adipocyte hypertrophy was shown to induce ER stress in an animal model [14]. ER stress has also been linked to the emergence of inflammation responses. ER stress activates JNK and IKK which are involved in signaling cascades [16, 17]. ER stress also leads to activation of CREB-H, which is a key regulator of inflammatory and acute-phase responses in the liver [18].

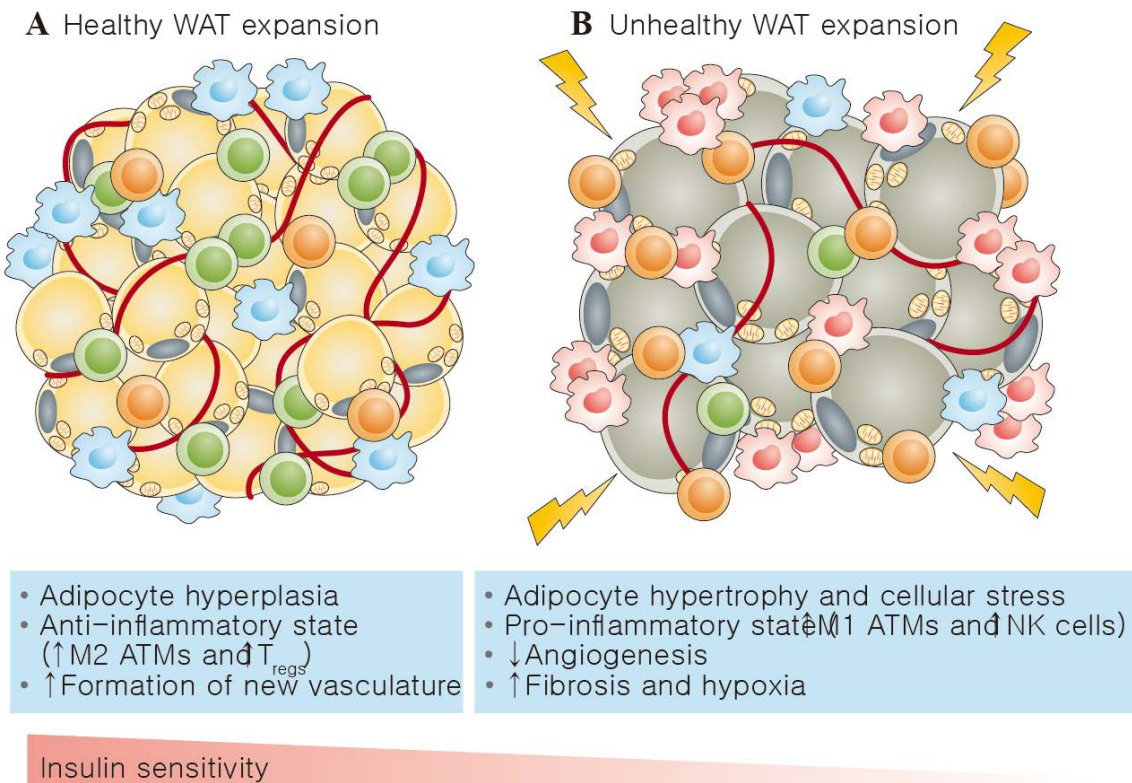


Figure 6. Healthy white adipose tissue expansion versus unhealthy pathological expansion in obesity [8]

3.2. Mitochondrial dysfunction and inflammation in adipocytes

In addition to the effects on the ER, obesity is associated with oxidative stress at the mitochondrial level. Because the ER is a major source of reactive oxygen species (ROS), oxidative stress, which is defined as an imbalance in the level of ROS and antioxidant defense, is induced in states of adiposity [19]. Oxidative stress in the mitochondria can induce cell damage, mutation of mitochondrial DNA, and apoptosis [20]. Notably, this apoptosis which induces the secretion of pro-inflammatory adipokines may lead to the attraction of pro-

inflammatory immune cells into adipose tissue, causing chronic and low-grade inflammation [21]. Recently, macrophage infiltration into adipose tissue was reported in obese conditions in both mouse and human models. Typically accompanied by chronic inflammation, obesity is associated with other metabolic syndromes such as cardiovascular disease, some types of cancer, and type 2 diabetes mellitus. Several studies found associations between insulin resistance and inflammation markers, such as increased production of leukocytes and concentrations of plasma interleukin-6 and tumor necrosis factor (TNF) α [22]. It was also reported that JNK-deficient mice were more resistant to obesity and insulin-sensitive than controls, suggesting that JNK, a potent target of TNF α -mediated-signaling, is a critical component of the regulatory pathway in obesity and insulin resistance *in vivo* [23]. Supporting the strong relationship between insulin resistance and type 2 diabetes, numerous markers of inflammation were found to be elevated in type 2 diabetes patients [24]. Other metabolic diseases, including hypertension and dyslipidemia, have also been linked to inflammatory cytokines and signal cascades [25]. Furthermore, it was reported that increased inflammation mediated by obesity is associated with hypertension and atherosclerosis [26].

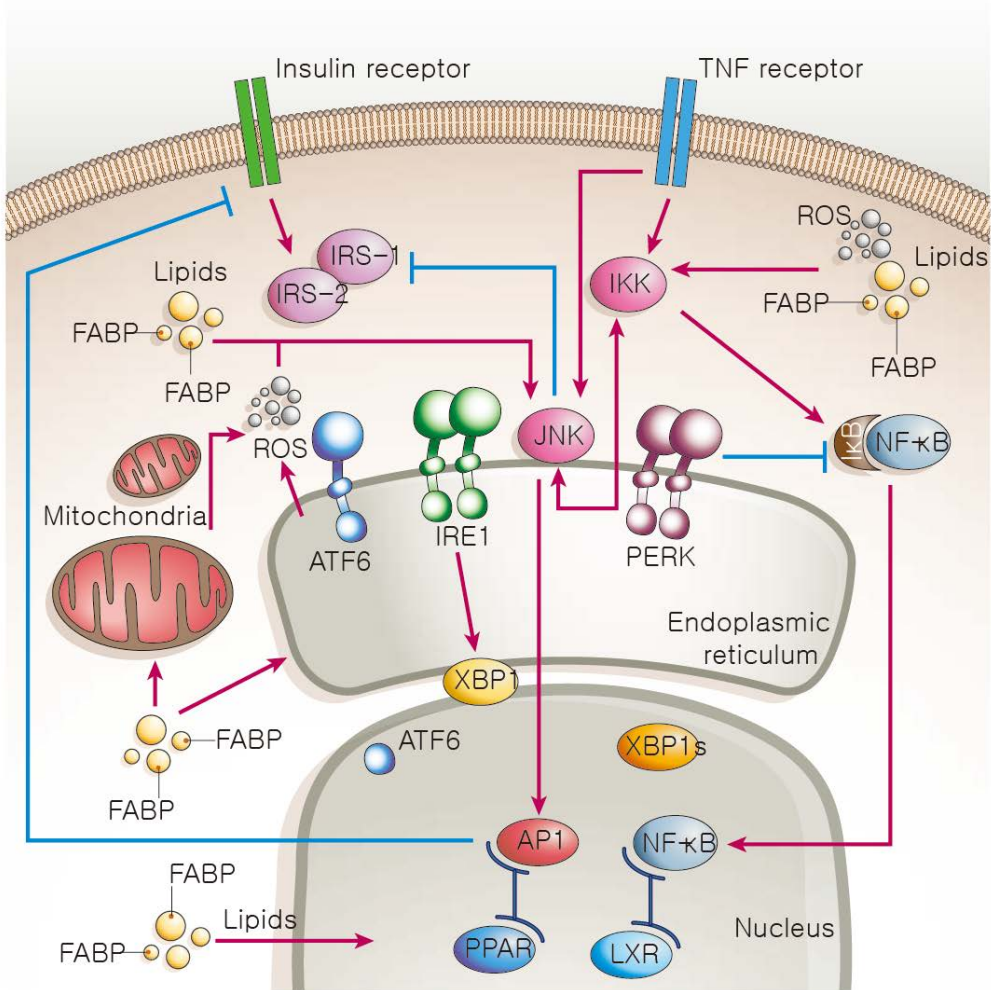


Figure 7. Molecular pathways of inflammatory responses with insulin action in adipocytes [8]

4. Therapeutic approaches for obesity

Lifestyle interventions including diet modification, physical activity, and behavior therapy are fundamental in the management of obesity [27]. Caloric restriction and sustained physical activity is the most important method of achieving and maintaining weight loss.

Adjunctive therapies in the form of pharmacotherapy and bariatric surgery are also considered for patients who do not achieve targeted weight loss goals or have a body mass index (BMI) above 30 [27]. However, pharmacotherapy options are limited by side effects and weight loss continues for only as long as the drug is being administered. Moreover, because of the limited efficacy of monotherapy, combination pharmacotherapy has been studied as a novel obesity treatment [28]. Bariatric surgery also has some disadvantages. Because bariatric surgery is permanent and irreversible, it should be thoughtfully considered for eligible patients. The risks associated with surgical procedures include infection, blood clots, gastrointestinal leakage, and lung problems. Long-term risks include malnutrition, ulcers, vomiting, and dumping syndrome, causing diarrhea, nausea, or vomiting [29, 30]. Thus, effective therapeutic options for obesity are urgently needed.

	BMI, kg/m ²			
	25.0–26.9	27.0–29.9	30.0–34.9	35.0–39.9≥40
Diet, physical activity, behavior therapy	Yes with comorbidities	Yes with comorbidities	Yes	Yes
Pharmacotherapy	No	Yes with comorbidities	Yes	Yes
Weight-loss surgery	No	No	Lap band with comorbidities	Yes with comorbidities

Abbreviation: BMI, body mass index.

Figure 8. Therapeutic strategies for obesity by BMI category [22]

5. UCP1 in brown adipocytes

5.1. Uncoupling protein 1

Uncoupling protein 1 (UCP1) is specifically expressed in the inner membrane of the mitochondria in BAT. The expression of UCP1 is linked to the unique thermogenic mechanism in BAT. In the 1960s, because of their lipid droplet form, brown adipocytes were considered as a subtype of adipocytes. However, a major difference between brown adipocytes and white adipocytes was demonstrated by electron microscopy [31]. Brown adipocytes contain unusual and numerous mitochondria with a hyper-developed inner mitochondrial membrane, known as the cristae [31]. The respiration of mitochondria is coupled to ADP phosphorylation to synthesize ATP [32]. However, BAT mitochondria can respire without phosphorylation of ADP, in contrast to the well-known energy conservation of mitochondria [33, 34]. Later, it was revealed that the unique respiratory mechanism of brown adipocytes depends on uncoupling proteins, particularly UCP1 [32].

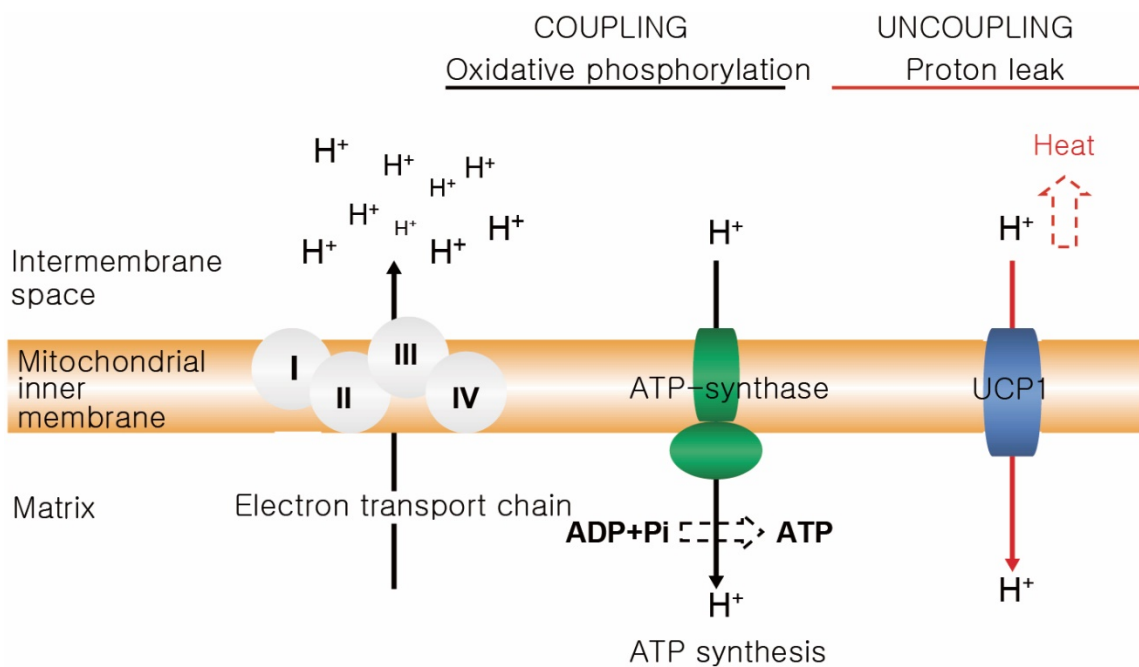


Figure 9. UCP1-mediated uncoupling of respiration from ATP synthesis [35]

5.2. Regulatory mechanism of UCP1 expression

The regulatory mechanism of UCP1 is now well-known [36]. Transcriptional regulation of UCP1 is controlled by members of the peroxisome proliferator-activated receptor (PPAR), CCAAT/enhancer-binding protein (CEBP) family, and cAMP response-binding protein (CREB) families. Adrenergic signaling for UCP1 expression involves a G-protein receptor mechanism coupled to cAMP production to induce phosphorylation of CREB and p38 MAPK in a protein kinase A-dependent manner. Phosphorylation of p38 MAPK is associated with the regulation of activating transcription factor 2, which promotes transcription of coactivator PGC1 α and UCP1. The interaction between retinoblastoma protein and FOXC2 is also related to the regulation of UCP1. More recently, PRDM16, which is dominantly expressed in brown adipocytes, was found to be essential for the induction of UCP1 expression through PGC1 α .

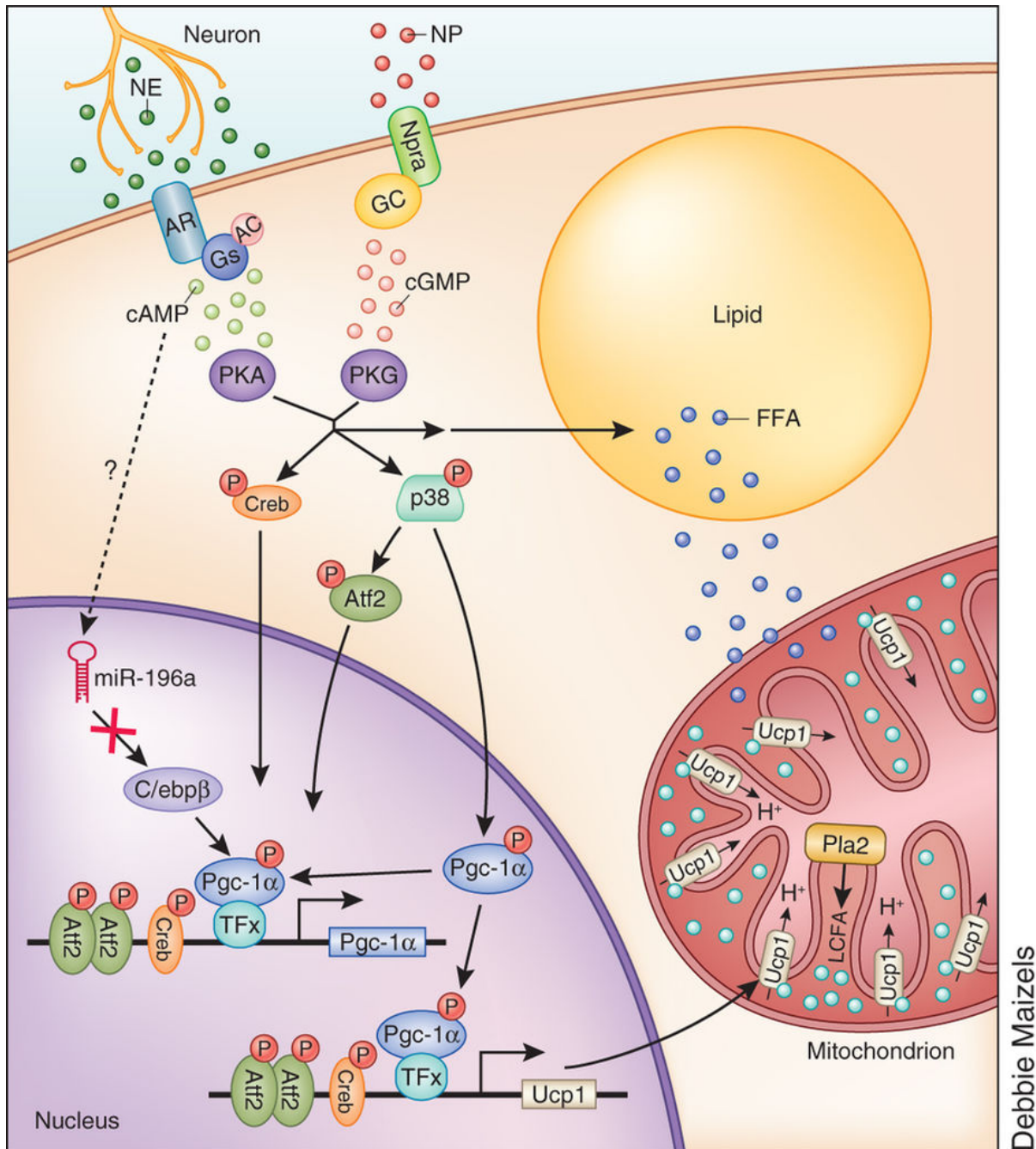


Figure 10. UCP1-mediated of thermogenesis in brown adipocytes [37]

6. White adipocyte browning

In recent years, the mechanism of adipogenesis was shown to be more dynamic than

previously believed [38]. It was thought that WAT predominates in adults, whereas most BAT is found only in the first few months of life [39]. However, adipose tissue, which is similar to BAT, is detected in adults when they are subjected to low temperatures for sympathetic stimulation [40]. Although some of the characteristics of this adipose tissue are as same as in BAT, it is likely that other characteristics correspond to adipose tissue variants including WAT. This type of adipose tissue has been named as brown-like adipose tissue [41-43]. Additionally, activation of the sympathetic nervous system, immune cells, and epigenetic modulators, which influence the transcriptional regulation of specific genes, may promote formation of brown-like adipocytes [44, 45]. Many clinical studies in human adults suggested that this activation of brown-like adipose tissue from WAT is beneficial [46]. Brown-like adipocytes in adults improved sensitivity to insulin and reduced body weight [47]. The reduction in glucose levels in the human serum along with an increase in insulin sensitivity is observed by inducing brown-like adipose tissue [46]. Thus, the promotion of brown-like adipocyte development in WAT shows important therapeutic potential for those who do not possess sufficient amounts of active BAT, such as the obese and elderly population.

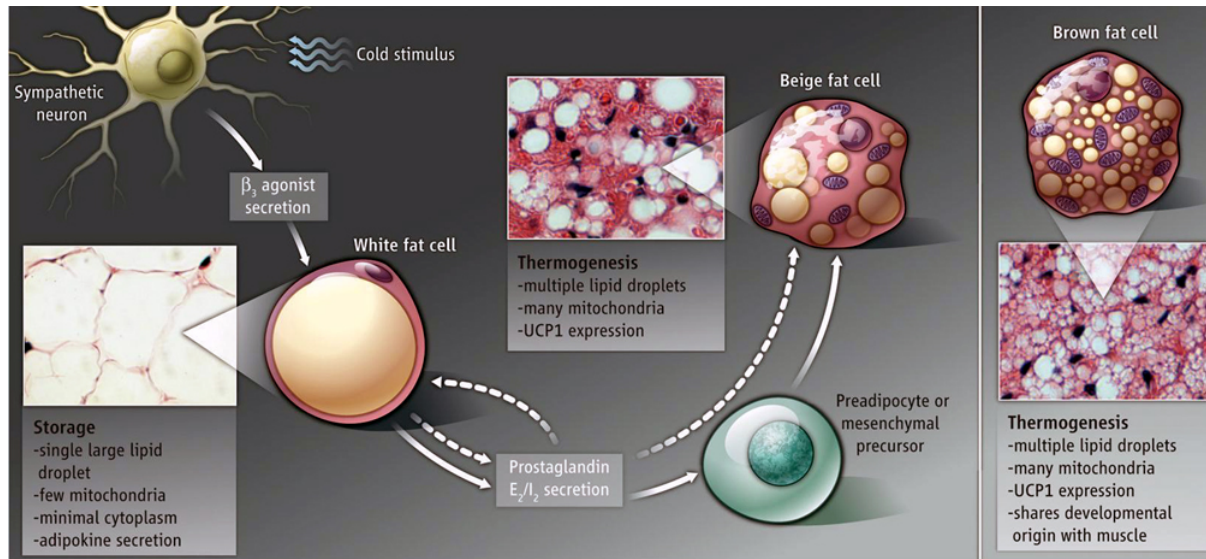


Figure 11. Cold-induced differentiation of brown-like/beige adipocytes [48]

7. Allicin: an active compound in garlic

7.1 Therapeutic properties of garlic

Garlic has been used as a food and medicine for a long time and has even been found in Egyptian pyramids [49]. In the Middle Ages, garlic was used as a therapeutic reagent for various diseases, including arthritis, toothache, parasitic infestation, snake and insect bites, and infectious disease [50]. Recently, several experimental and clinical investigations demonstrated the therapeutic effects of garlic. These effects include the reduction of risk factors of cardiovascular diseases and cancer, antioxidant effects, and antimicrobial effects [51, 52]. Particularly, various reports demonstrated that garlic lowered plasma lipid levels, although some reports have questioned the bioavailability of garlic [53, 54]. Garlic reduced the plasma concentration of triglycerides, free fatty acids, total cholesterol, and leptin. Moreover, liver

triglycerides and total cholesterol were reduced by garlic administration in mice [55]. These beneficial effects of garlic could be attributed to its diverse organosulfur compounds including allicin and its metabolites. The name allicin originates from the Latin name of garlic, Allium sativum L., in the family of Liliaceae [56]. The levels of allin, the precursor of allicin, and allicin differ depending on the variety of garlic [57] and form of garlic supplement [58]. It has been reported that allicin is further metabolized to produce diallyl sulfide, diallyl disulfide, diallyl trisulfide, allyl methyl trisulfide, dithiin, ajoene, and vinyl dithiin [59, 60]. Ajoene induces apoptosis and inhibits lipid accumulation in white adipocyte cell lines [61]. Additionally, vinlydithiin inhibits the differentiation of human adipocytes [62]. Allicin also has cholesterol-lowering effects in mice. These anti-obesity actions of organosulfur compounds derived from garlic may critically contribute to the anti-obesity and anti-lipogenic effects of garlic.

7.2 Antioxidant and anti-inflammatory effects of allicin

Allicin is one of the most widely studied natural compounds. It has been reported that allicin has antioxidant and anti-cancer activities as well as anti-hypercholesterolemia activity. In endothelial cells, allicin lowered ROS production, which can lead to oxidative stress-induced damage to biological macromolecules and structure, such as the mitochondria, and promoted glutathione production [63]. Oral administration of allicin prevented ROS-induced cardiac hypertrophy by inhibiting the mitogen-activated protein kinase (MAPK) and phosphoinositide 3-kinase/AKT/glycogen synthase kinase 3 β signaling pathways [64]. Allicin-induced generation of nitric oxide (NO) has protective effects against oxidative and inflammatory damage in endothelial cells [65]. Allicin has also been reported to have anti-cancer effects. In

normal cells, the cell cycle is tightly regulated. When DNA damage or defects in DNA replication occurs, the cell cycle can be arrested to repair the error [66]. Apoptosis is triggered when DNA repair fails. However, cancer can evade apoptosis, resulting in unregulated proliferation of cancer cells [66]. It has been reported that the inflammatory responses, particularly the nuclear factor- κ B-related signal pathway, are important in the mechanism of evading apoptosis [67]. Though this tumor evasion mechanism, allicin can induce cell cycle arrest in cancer cell lines. Moreover, allicin treatment can lead to apoptosis in various types of cancer cells *in vitro* [68, 69]. Indeed, allicin inhibits the activation of nuclear factor- κ B and production of induced nitric oxide synthase and TNF α in lipopolysaccharide-treated mouse macrophage, suggesting that allicin regulates pro-inflammatory signal pathways [70, 71]. Because oxidative stress results in the dysfunction and low-inflammatory status of adipocytes in obesity, these antioxidant and anti-inflammatory effects of allicin may contribute to the anti-obesity effects of allicin. However, the bioactivity of allicin towards adipocytes is not fully understood. Although allicin enhances thermogenesis by increasing UCP content in BAT [72], the exact mechanism by which allicin induces the formation of brown-like adipocytes is unclear.

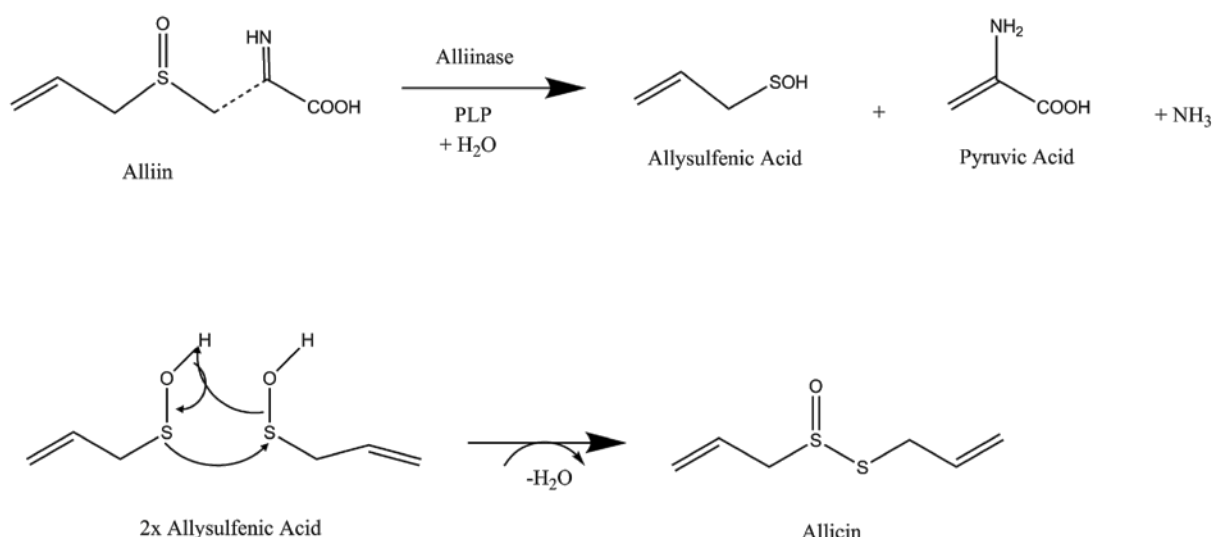


Figure 12. Biosynthesis of allicin

8. KLF 15

Krüppel-like factors (KLFs) are a subclass of the zinc-finger family of transcriptional regulators. The transcriptional functions of KLF family members as activators or repressors depend on the promoters to which they bind and coactivators via interactions [73, 74]. Particularly, KLF15 was the first identified protein that binds to the promoter of CLC-K1, a kidney-specific CLC chloride channel gene [75]. It has been reported that KLF15 regulates gene expression in various cell types, including adipocytes [76]. In obese mice, overexpression of KLF15 in adipose tissue resulted in resistance to obesity, suggesting that KLF15 is a key factor in the regulatory mechanism of adipose tissue [77]. It was also found that KLF15 enhanced the expression of UCP1 by interacting with the UCP1 promoter region in brown adipocytes [78]. However, despite intensive studies investigating the role of KLF15 in BAT, little is known about its mechanism of action in the adipocyte browning mechanism in WAT.

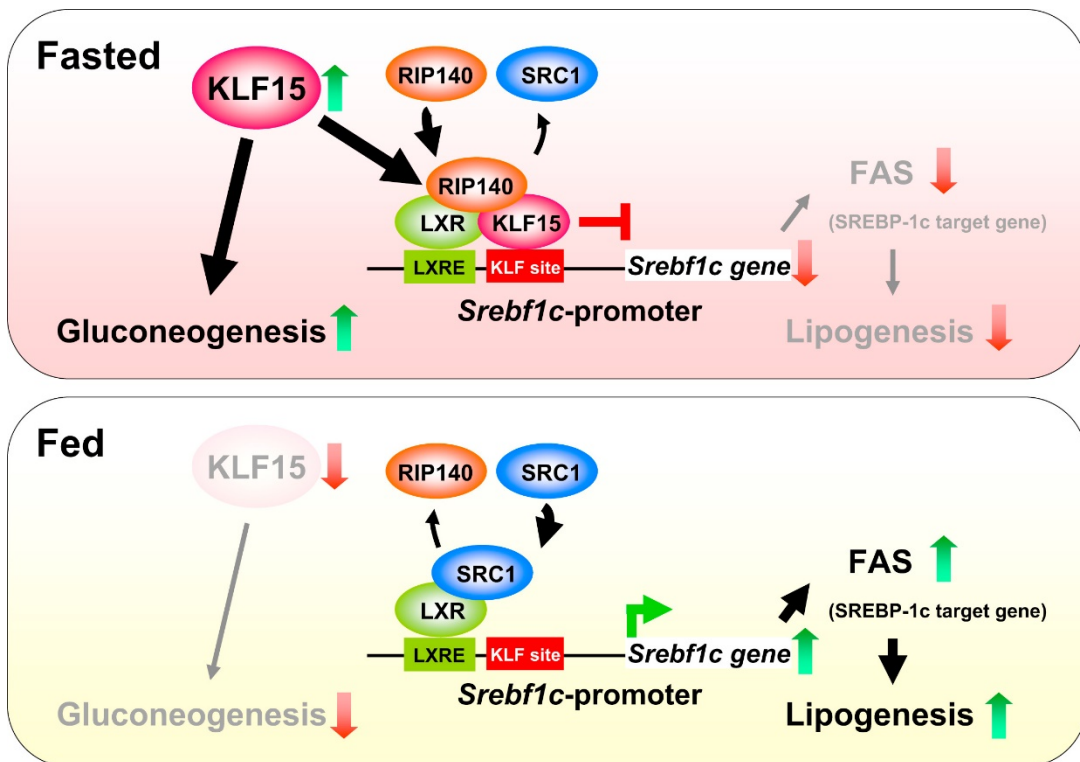


Figure 13. Regulatory mechanism of KLF15 on switching between lipogenesis and gluconeogenesis during fasting [79]

9. Aim of study

In obesity, WAT dysfunction results in hypertrophy-related excessive lipid accumulation and low-inflammatory conditions, which reduces insulin sensitivity and may cause metabolic diseases. Although pharmacological therapy and bariatric surgery offer some relief, these treatments are costly and show side effects. Therefore, the demand for more effective, nonsurgical, and pharmacological therapies is increasing. Notably, brown-like adipocytes have received attention because of their ability to increase energy expenditure and potential to be generated from white adipocytes. The aim of study was to identify whether allicin induces white adipocyte browning and investigate the allicin-induced cellular

mechanism of white adipocyte browning if allicin has browning effects. The present data demonstrated the anti-obesity and browning effects of allicin in differentiated 3T3-L1 cells, mouse inguinal adipose tissue (iWAT), and iWAT stromal vascular cells (SVCs). Although the precise role of KLF15 in the browning mechanism of white adipocyte was unknown, the data demonstrated that allicin-induced UCP1 expression was regulated though KLF15 involved in a signaling cascade.

II. MATERIAL AND METHODS

1. Materials

1.1 Chemicals

3-Isobutyl-1-methylxanthine (IBMX)	Sigma-Aldrich Co., MO, USA
Agarose E	Sigma-Aldrich Co., MO, USA
Acrylamide/Bis-acrylamide (29:1)	Sigma-Aldrich Co., MO, USA
Aminoacetic persulfate (APS)	Sigma-Aldrich Co., MO, USA
Ammonium acetate	Sigma-Aldrich Co., MO, USA
Ammonium chloride	Sigma-Aldrich Co., MO, USA
Anti-β-actin monoclonal antibody	Santa Cruz Biotechnology, Inc., TX, USA
Anti-ERK polyclonal antibody	Cell Signaling Technology, MA, USA
Anti-JNK polyclonal antibody	Cell Signaling Technology, MA, USA
Anti-KLF15 monoclonal antibody	Santa Cruz Biotechnology, Inc., TX, USA
Anti-UCP1 monoclonal antibody	Santa Cruz Biotechnology, Inc., TX, USA
Anti-goat IgG	Santa Cruz Biotechnology, Inc., TX, USA
Anti-mouse IgG	Santa Cruz Biotechnology, Inc., TX, USA
Anti-p38 polyclonal antibody	Cell Signaling Technology, MA, USA
Anti-phospho ERK polyclonal antibody	Cell Signaling Technology, MA, USA

Anti-phospho JNK polyclonal antibody	Cell Signaling Technology, MA, USA
Anti-phospho p38 polyclonal antibody	Cell Signaling Technology, MA, USA
Anti-rabbit IgG	Santa Cruz Biotechnology, Inc., TX, USA
Bovine serum albumin (BSA)	Sigma-Aldrich Co., MO, USA
Bromophenol blue	Sigma-Aldrich Co., MO, USA
Chloroform	Sigma-Aldrich Co., MO, USA
DC protein assay	Bio-Rad Laboratories. Inc., CA, USA
Dexamethasone	Sigma-Aldrich Co., MO, USA
Dimethyl sulfoxide (DMSO)	Sigma-Aldrich Co., MO, USA
1,4-Dithiothreitol (DTT)	Sigma-Aldrich Co., MO, USA
Dulbecco's modified eagle medium	Life Technologies, CA, USA
DMEM	Life Technologies, CA, USA
Ethanol	Sigma-Aldrich Co., MO, USA
Ethylenediaminetetraacetic acid (EDTA)	Sigma-Aldrich Co., MO, USA
Ethylene glycol-bis (2-aminoethylether)-	Sigma-Aldrich Co., MO, USA
N,N,N',N'-tetraacetic acid (EGTA)	
Fetal bovine serum (FBS)	Biotechnics Research Inc, CA, USA
Fetal calf serum (FCS)	Life Technologies, CA, USA
GelRed	Koma Biotech., Korea
GeneRuler DNA ladder	Fermentas, MA, USA
Glycerol	Sigma-Aldrich Co., MO, USA
Glycine	Sigma-Aldrich Co., MO, USA
4-(2-Hydroxyethyl) piperazine-1-	Sigma-Aldrich Co., MO, USA
Ethanesulfonic acid (HEPES)	

Indomethacin	Sigma-Aldrich Co., MO, USA
Insulin	Sigma-Aldrich Co., MO, USA
Leupeptin	Sigma-Aldrich Co., MO, USA
Magnesium chloride	Sigma-Aldrich Co., MO, USA
Metafectene	Biontex, CA, USA
Methanol	Sigma-Aldrich Co., MO, USA
MitoTracker Red CMXRos	Invitrogen, CA, USA
Nitrocellulose (NC) membrane	Millipore Corp., MA, USA
Oil Red O	Sigma-Aldrich Co., MO, USA
Opti-protein marker	Applied Biological Materials Inc., BC, Canada
Penicillin-Streptomycin	Biotechnics Research Inc, CA, USA
Pepstatin A	Sigma-Aldrich Co., MO, USA
Phenylmethanesulfonyl fluoride (PMSF)	Sigma-Aldrich Co., MO, USA
Phosphate-buffered saline (PBS)	Biotechnics Research Inc, CA, USA
Potassium chloride	Sigma-Aldrich Co., MO, USA
Propidium iodide (PI)	Sigma-Aldrich Co., MO, USA
Protein A/G PLUS-agarose	Santa Cruz Biotechnology, Inc., TX, USA
Proteinase K	Sigma-Aldrich Co., MO, USA
Polyoxethylenesorbitan monolaurate (Tween 20)	Daejung Chemical & Metal Co. Ltd, Korea
Polyvinylidene difluoride (PVDF) membrane	Millipore Corp., MA, USA
Ribonuclease A (RNase A)	Calbiochem, MA, USA

Skim milk	Millipore Corp., MA, USA
Sodium chloride	Sigma-Aldrich Co., MO, USA
Sodium dodecyl sulfate (SDS)	Sigma-Aldrich Co., MO, USA
Sodium deoxycholate Sucrose	Sigma-Aldrich Co., MO, USA
SYBR® Green Real-Time PCR Master Mix	BioLegned, Inc., USA
N,N,N',N'-tetramethylmethylenediamine (TEMED)	Sigma-Aldrich Co., MO, USA
Tris (hydroxymethyl) aminomethane (Tris-base)	Daejung Chemical & Metal Co. Ltd, Korea
Trizol	Invitrogen, CA, USA
Trypsin-EDTA	Sigma-Aldrich Co., MO, USA
WB detection reagent kit	Amersham, UK

1.2. Instruments

Autoclave	HYSC, Korea
Balance	A&D Engineering, Inc., CA, USA
Cell culture centrifuge	Sigma Laborzentrifugen GmbH, Germany
CLAMS	Columbus Instruments, OH, USA
CO ₂ incubator (water-jacketed)	NuAire, MN, USA
Davinch-chemi TM Chemiluminescence	Celltagen Co., LTD., KOREA
Imaging System	
DNA image visualizer (MyImager)	Seoulin Bioscience Co., Ltd., Korea
Freezer	Thermo Fisher Scientific Inc., MA, USA

GeneAmp PCR system 2400	Applied Biosystems, CA, USA
Hot plate/magnetic stirrer	Vision Scientific Co, Ltd., Korea
Inverted microscope	Olympus, Japan
Microcentrifuge (Gyrogen 1740R)	JEIO Tech., Korea
Microplate mixer	BMS Co., Ltd., Korea
Microplate reader	Scientific Industries, Inc., NY, USA
Orbital shaker	Molecular Devices, CA, USA
pH meter (benchtop)	Thermo Fisher Scientific Inc., MA, USA
Power supply	ATTO Corp., Japan
RunOne TM electrophoresis cell	ATTO Corp., Japan
Semi-dry transfer system (HorizeBLOT)	ATTO Corp., Japan
Thermal cycler (PCR machine)	ATTO Corp., Japan
Thermomixer	Applied Biosystems, CA, USA
UV-spectrophotometer	Eppendorf AG, Hamburg, Germany
Vortex mixer	Shimadzu, Corp., Japan
Water bath	Scientific Industries, Inc., NY, USA

2. Methods

2.1. Reagents and purification of allicin

Unless otherwise indicated, all chemicals were purchased from Sigma Chemical Co. (St Louis, MO, USA). Penicillin G, streptomycin, and fetal bovine serum (FBS) were obtained

from Biotechnics Research Inc (Irvine, CA, USA). The Bio-Rad DC protein assay kit was obtained from Bio-Rad (Hercules, CA, USA). Antibodies against extracellular signal-regulated kinase (ERK), phospho-ERK, p38, phospho-p38, c-Jun N-terminal kinase (JNK), and phospho-JNK were supplied by Cell Signaling Technology (Danvers, MA, USA). Antibodies against KLF15, UCP1, and β -actin were purchased from Santa Cruz Biotechnology (Dallas, TX, USA). The enhanced chemiluminescence kit was obtained from Amersham (Amersham, UK). TRIzol reagent and the SuperScript II cDNA synthesis kit were purchased from Invitrogen (Carlsbad, CA, USA).

2.2. Cell culture and differentiation

3T3-L1 pre-adipocytes were purchased from American Type Culture Collection (ATCC; Manassas, VA, USA). The pre-adipocytes were maintained in Dulbecco's modified Eagle's medium (DMEM; Life Technologies, Carlsbad, CA, USA) supplemented with 10% newborn calf serum (Life Technologies) and antibiotics (Lonza, Basel, Switzerland) at 37°C in 5% CO₂. To induce adipocyte differentiation, 3T3-L1 cells were plated at a density of 2 \times 10⁵ cells per well into 6-well plates. After reaching confluence, the cells were incubated in DMEM supplemented with 10% FBS (Life Technologies) and antibiotics. The cells were treated with MDI (1 μ M dexamethasone (Sigma-Aldrich) and 0.5 mM 3-iso-butyryl-1-methylxantine (Sigma-Aldrich) and 10 μ g/mL insulin (Sigma-Aldrich)) for 2 days followed by treatment with insulin alone. To investigate the effects of allicin on the differentiation of adipocytes, allicin concentrations of 1, 10, and 100 ng/mL were supplemented at 2-day intervals when the medium was replenished. The cells were transferred into DMEM containing 10% FBS for the remaining culture period. The cultures were replenished every 2 days. After induction for 10 days, more

than 90% of the cells exhibited the typical adipocyte morphology.

SVCs were isolated from iWAT as previously described [29]. The medium was changed every other day. To induce brown adipogenic differentiation of SVCs, confluent SVCs were cultured in DMEM/F12 containing 10% FBS, 1% penicillin–streptomycin solution with 5 µg/mL insulin, 1 nM T3, 1 µM dexamethasone, 0.5 mM 3-isobutyl-1-methylxanthine, and 0.125 mM indomethacin for 2 days. The cells were switched to DMEM/F12 supplemented with 10% FBS and 5 µg/mL insulin for 5 additional days, and the medium was changed every 2 days.

2.3 Animals

Male 4-week-old C57BL/6J mice were purchased from SLC, Inc. (Hamamatsu, Japan). Upon arrival, the mice were fed a normal-fat diet (NFD) for 1 week, after which they were fed a high-fat diet (HFD) containing 60% fat (Research Diets, Inc., New Brunswick, NJ, USA). One group was orally administered 100 mL PBS every 2 days as a negative control. The remaining mice were orally administered 100 mL containing 1 mg/kg allicin every 2 days. Food intake and body weight were monitored weekly for 8 weeks. Mice were housed in environmentally controlled rooms with a 12-h light–dark cycle and free access to food and water. Before and after treatment, the basal metabolic rate [oxygen consumption (VO₂), CO₂ production (VCO₂), and respiratory exchange ratio (RER)] of mice during the day (quiescent phase) was measured using a CLAMS (Columbus Instruments, Columbus, OH, USA) indirect open circuit calorimetry system. Blood was drawn from the abdominal aorta into an ethylenediamine tetra-acetic acid (EDTA)-coated tubes, and the serum was obtained by

centrifugation at 2000 rpm for 15 min at 4°C. Body weight and food intake were measured weekly. At the end of the 8 weeks of treatment, mice were sacrificed by CO₂ anesthesia. The iWAT was rapidly isolated and weighed. One side of the adipose tissues was frozen in liquid nitrogen and stored at -80°C until further analyses. A middle portion of the other side was fixed in 4% paraformaldehyde for sectioning and staining. This study was approved by the animal care and use committee of Sungkyunkwan University.

2.4. Isolation of total RNA and quantitative real-time PCR

Following the manufacturer's protocol, total RNA was extracted from iWAT isolated from HFD-fed mice or HFD-fed mice orally administered allicin and from 3T3-L1 cells using TRIzol reagent. Isolated RNA (1 mg/mL) was reverse-transcribed using a SuperScript II kit for cDNA synthesis. The generated cDNA was subjected to real-time reverse transcription (RT)-PCR reactions using thermocyclers from Applied Biosystems (Foster City, CA, USA) or Stratagene (La Jolla, CA, USA). In real-time RT-PCR, diluted cDNA was added to SYBR mix containing 100 ng/mL PCR primers. Reaction conditions were as follows: 95°C for 10 min, 40 cycles of 95°C for 10 s (melting), and 60°C for 1 min (annealing and elongation). Melting curve analyses from 76°C to 84°C were performed at the end of each run as a quality control step. The cDNA was subjected to quantitative real-time (qRT)-PCR using thermocyclers from Applied Biosystems. Primer sequences corresponding to the mouse adipogenic genes analyzed in this study are shown in Table 1.

Gene	Forward primer (5'- 3')	Reverse primer (5'- 3')
PRDM16	CAGCACGGTGAAGCCATT	GCGTGCATCCGCTTGTG
PGC1 α	CCCTGCCATTGTTAAGACC	TGCTGCTGTTCTGTTTC
UCP1	ACTGCCACACCTCCAGTCATT	CTTGCCCTCACTCAGGATTGG
GAPDH	TGCATCCTGCACCAACCAA	TCCACGATGCCAAAGTTGTC

Table 1. Primer sequences and real-time PCR conditions

2.5 Determination of lipid accumulation by Oil Red O staining

3T3-L1 cells (8×10^4 cells/well) were plated into 96-well plates and maintained for 2 days after reaching confluence. The media was exchanged with differentiation medium (DMEM containing 10% FBS, 1 μ M dexamethasone, 0.5 mM IBMX, 10 μ g/mL insulin) and the cells were treated with allicin (1, 10, 100 ng/mL). Oil Red O staining was performed at 6 days to stain the accumulated lipid droplets in differentiated adipocytes. The cells were washed with phosphate-buffered saline, fixed with 10% formalin for 10 min, and incubated with 60% (wt/wt) filtered Oil Red O (Sigma) in 100% isopropanol for 1 h at room temperature. After removing the staining solution, the stained cells were washed three times with distilled water to remove excess dye and photographed under a microscope. To quantify intracellular lipid accumulation, the stained lipid droplets were dissolved with 100% isopropanol for 10 min. The optical density was measured at 490 nm with a spectrophotometer.

2.6. Mitotracker staining and confocal laser microscopy

MitoTracker Red CMXRos (Invitrogen), a mitochondria-specific cationic fluorescent dye, was used to label the mitochondria. The transfected 3T3-L1 adipocytes on the tenth day of differentiation were incubated with 150 nM MitoTracker for 30 min at 37°C and washed three times with pre-warmed PBS. Cells were imaged using a confocal laser scanning microscope (Zeiss, Gottingen, Germany).

2.7. Western blot analysis

Total cell lysates were prepared using RIPA buffer (150 mM NaCl, 50 mM Tris-HCl pH 8.0, 5 mM EDTA, 1% sodium deoxycholate, 0.1% SDS, and 1% Triton X-100) supplemented with protease inhibitors before use. Protein concentrations were quantified using the DC protein Assay (Bio-Rad). Aliquots (15–30 µg of protein) of cell lysates were resolved by SDS-PAGE, followed by transfer of the proteins to nitrocellulose or polyvinylidene fluoride membranes (Millipore Corp., Billerica, MA, USA). After blocking with 5% skim milk in Tris-buffered saline containing 0.05% Tween-20 (TBST) was added and the membrane was incubated for 2 h at room temperature. The membrane was probed overnight at 4°C with primary antibody diluted in phosphatase-buffered saline containing 0.1% Tween-20 (PBST). After several washes with TBST, the membrane was incubated with the appropriate horseradish peroxidase-conjugated secondary antibody diluted in PBST at room temperature for 1 h. After the final washes, the immunocomplex was developed using a chemiluminescence kit. After measuring the intensity of each band by densitometry using the image processing software ImageJ (NIH, Bethesda, MD, USA), the relative intensities were calculated by normalizing to the levels of β-actin from the corresponding sample.

The fractionated proteins were probed with antibodies to ERK, phospho- ERK, p38, phospho-p38, JNK, phospho- JNK, UCP1, KLF15, and β -actin. In all immunoblotting experiments, the blots were re-probed with an anti- β -actin antibody as a control for protein loading.

2.8. siRNAs

The mouse KLF15 (mixture of Stealth select siRNAs: 5'-GGAGGUUGAACUUG-GACGGGAGUUU-3', 5'-CCUCCUUGUAAAGACGAAGGGACUU-3') and control siRNA (Stealth RNAi Negative Control High GC Duplex) were purchased from Invitrogen. The siRNAs were transfected using Lipofectamine RNAiMAX reagent (Invitrogen).

2.9. Chromatin immunoprecipitation assay

Differentiated 3T3-L1 cells were cross-linked for 10 min by adding formaldehyde directly to the tissue culture medium at a final concentration of 1% at room temperature. Mice iWAT were dissected and washed twice with PBS, minced, and homogenized before cross-linking. Cross-linking was stopped by adding glycine at a final concentration of 0.125 M. Cross-linked liver samples were dounced on ice with a B douncer six times to disaggregate the hepatocytes, washed twice with cold 1× phosphate-buffered saline, and swelled in RSB buffer (3 mM MgCl₂, 10 mM NaCl, 10 mM Tris-chloride [pH 7.4], in the presence of 0.1% NP-40 and protease inhibitors [0.5 mM phenylmethylsulfonyl fluoride, 100 ng of leupeptin per ml,

100 ng of aprotinin per mL]). The samples were dounced again on ice 10 additional times to aid in nuclei release. Nuclei were pelleted by centrifugation and resuspended in nuclei lysis buffer (1% sodium dodecyl sulfate, 10 mM EDTA, 50 mM Tris-chloride [pH 8.1] plus protease inhibitors). The resulting chromatin solution was sonicated for 15 10-s pulses at maximum power. Four primary aliquots from each cross-linked liver were obtained. After centrifugation, the supernatant of one aliquot was precleared with blocked protein A-positive Staph cells (Roche, Basel, Switzerland), diluted 1:3 with dilution buffer (0.01% sodium dodecyl sulfate, 1.1% Triton X-100, 1.2 mM EDTA, 16.7 mM Tris-chloride [pH 8.1], 167 mM NaCl, and protease inhibitors) and divided into aliquots. Anti-KLF15 antibody or 5 µL of IgG antibody was added to each aliquot of chromatin and incubated on an oscillating platform for 16 h at 4°C. Another aliquot was incubated with no antibody. Antibody-protein-DNA complexes were isolated by immunoprecipitation with preblocked protein A-positive Staph A cells; after extensive washing, the complexes were eluted. Following addition of NaCl to a final concentration of 0.3 M and 1 µl of RNase A (10 mg/mL), the samples were incubated in a 67°C water bath to reverse the formaldehyde cross-linking. After digestion with proteinase K, the samples were extracted with phenol-chloroform-isoamyl alcohol and chloroform-isoamyl alcohol. DNA was precipitated and resuspended in water. Samples were analyzed by PCR using 1/10 of the sample and suitable primers. Immunoprecipitated DNA was amplified by PCR using primers specific for the UCP1 promoter, sense, 5'-AAAAGTGACCACAC-GATG-3' and antisense, 5'-CTGCGCCCTGACCTGGGA -3'.

2.10. Immunohistochemistry

For histological analysis, adipose tissue was fixed in 4% formaldehyde and embedded in paraffin. Paraffin-embedded iWAT sections (5- μ m thickness) were stained with hematoxylin and eosin (H&E). Immunohistochemistry was performed using the Vectastain Elite ABC kit (Vector Laboratories, Burlingame, CA, USA) according to the manufacturer's instructions using anti-UCP1 antibody (Abcam, Cambridge, UK) and anti-KLF15 antibody (Acris Antibodies, Herford, Germany) (1:1000).

2.11. Statistical analysis

Each experiment was repeated at least three times, and the results of a representative experiment are shown. Each result is reported as the mean \pm standard error of the mean. One-way analysis of variance was used to determine the significance among groups, after which a modified t-test with Bonferroni correction was used for comparison between individual groups. P < 0.05 was considered statistically significant.

III. RESULT

1. Effect of allicin on expression of brown adipocyte-selective genes in white adipocytes

To investigate whether allicin has a browning effect in white adipocytes, the mRNA expression of genes that regulate the bioactivity of brown adipocytes in differentiated 3T3-L1 cells was analyzed by RT-PCR. As shown in Figure 14, allicin significantly increased the mRNA levels of brown adipocyte-selective genes, including PRDM16, PGC1 α , and UCP1 in differentiated 3T3-L1 cells.

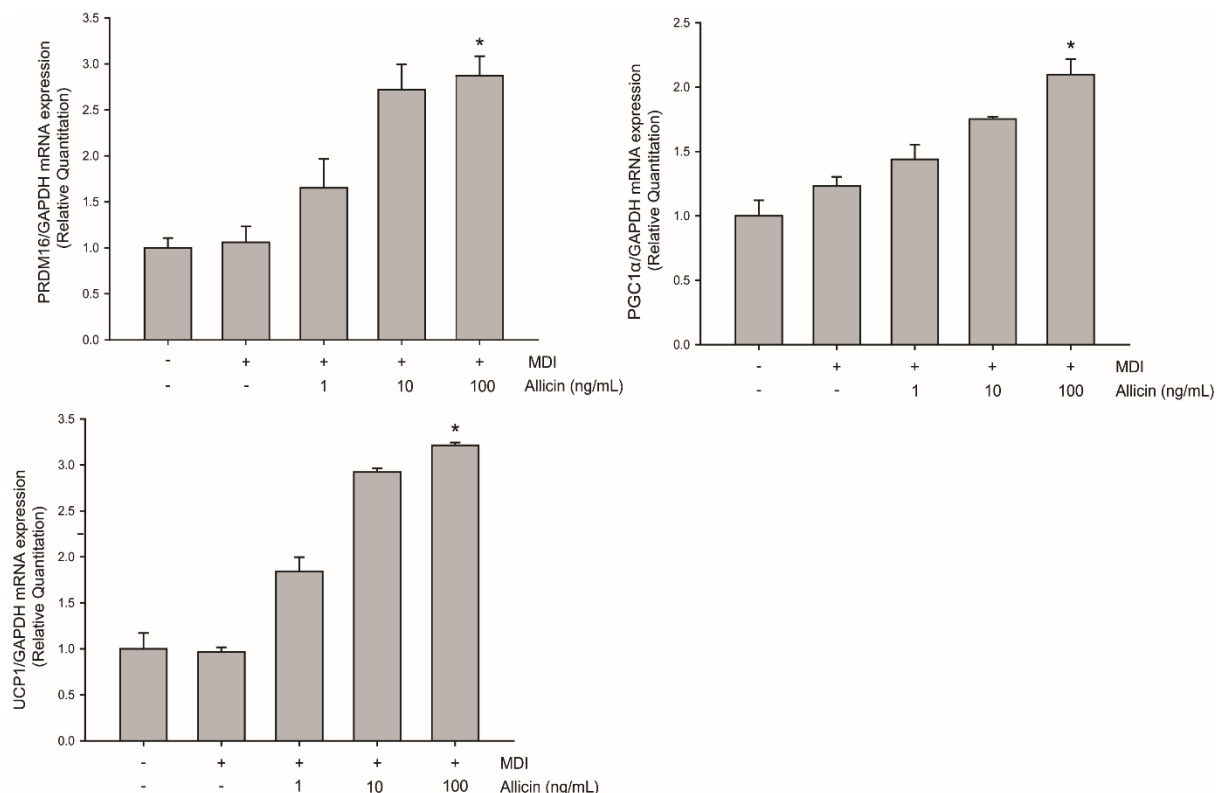
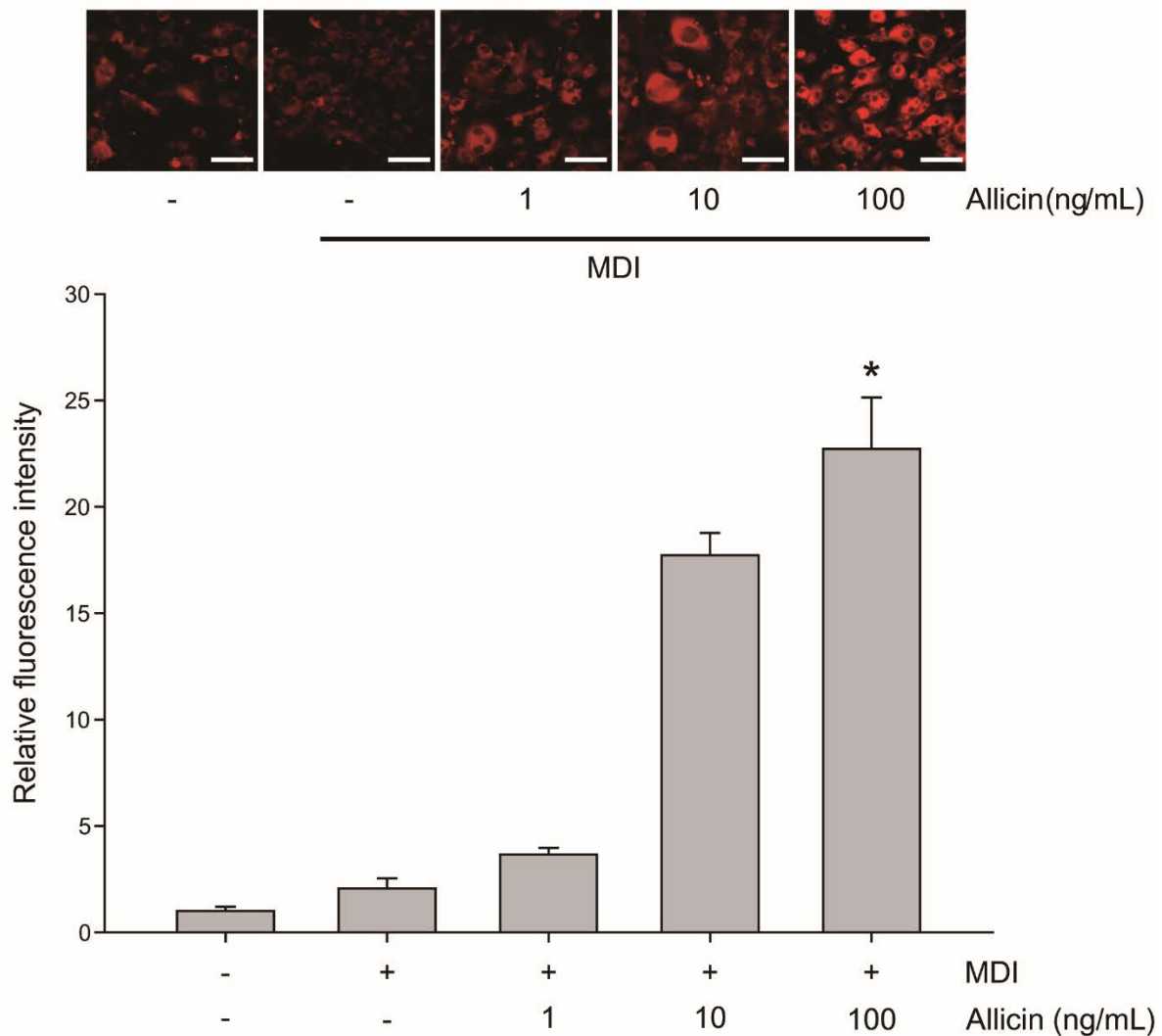


Figure 14. Effect of allicin on expression of brown adipocyte-selective genes in white

adipocytes. Relative mRNA expression of brown adipocyte-selective genes (PRDM16, UCP1, and PGC1 α) in MDI-induced 3T3-L1 cells at the indicated concentration of allicin for 7 days. Data are expressed as the means \pm S.E.M. of three independent experiments.*P < 0.05, significantly different from MDI-treated cells.

2. Effect of allicin on accumulation of mitochondria in white adipocytes

Brown adipocytes are mitochondria-rich cells and the increased accumulation of mitochondria is typical sign of adipocyte browning. Therefore, in order to measure mitochondrial mass in differentiated 3T3-L1 cells, Mito Tracker fluorescence analysis was performed under confocal microscopy. As shown in Figure 15A, allicin-treated 3T3-L1 cells were stained strongly in a concentration dependent manner, indicating allicin-induced mitochondrial biogenesis. However, allicin did not modulate adipogenic differentiation in 3T3-L1, because Oil-Red O staining result demonstrated that the lipid accumulation of 3T3-L1 was not significantly affected by allicin treatment (Fig. 15B).

A

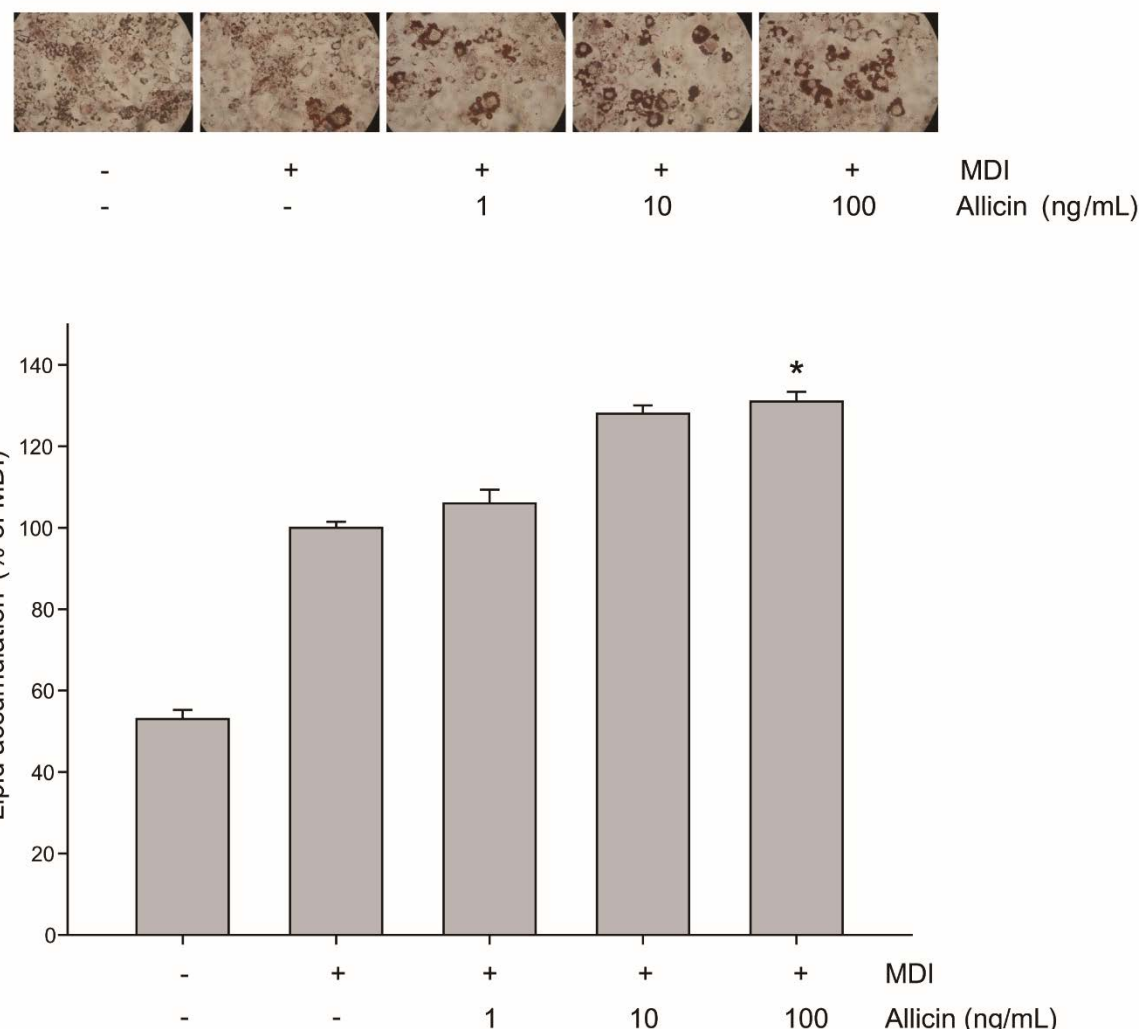
B

Figure 15. Effect of allicin on the accumulation of mitochondria in white adipocytes. (A) Differentiated 3T3-L1 cells were stained with MitoTracker Red. Mitochondrial morphology was analyzed by using confocal microscopy. Scale bar, 10 mm. The bar graph represents the percentage of cell populations with fragmented mitochondria. (B) Differentiated 3T3-L1 cells with visible lipid accumulations were observed by Oil red O staining at 8 days. Lipid accumulation was quantified with a micro-reader at 490 nm. Data are expressed as the means \pm S.E.M. of three independent experiments. * $P < 0.05$, significantly different from MDI-treated cells.

3. Effect of allicin on KLF15 expression in white adipocytes

KLF15 is a transcriptional factor that plays a critical role in brown adipocyte differentiation and regulates the expression of the brown adipocyte marker UCP1 [78]. To understand the regulatory mechanisms of allicin on white adipocyte browning, the effect of allicin on the protein expression of KFL15 was investigated. As shown in Figure 16, the protein expression of KLF15 was up-regulated by allicin in differentiated 3T3-L1 cells. Consistent with the mRNA expression, the protein expression of UCP1 protein was significantly up-regulated. Similar protein expression patterns for KLF15 and UCP1 were observed in differentiated inguinal WAT (iWAT) stromal vascular cells (SVCs). KLF15 and UCP1 expression was induced by allicin treatment.

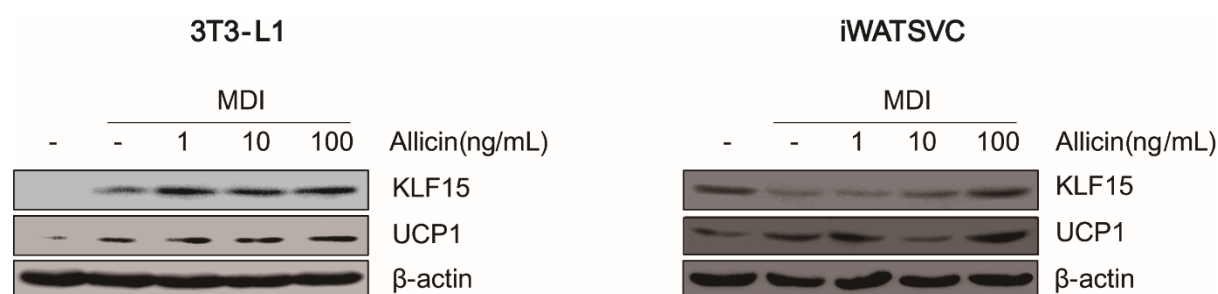


Figure 16. Effect of allicin on KLF15 expression in white adipocytes. 3T3-L1 preadipocytes and iWAT SVCs were cultured in differentiation medium containing 1, 10, and 100 ng/mL of allicin. The protein levels of KLF15 and UCP1 were determined in differentiated 3T3-L1 cells or iWAT SVCs by western blot analysis. β-actin protein level was considered as an internal control. A typical result obtained from three independent experiments is shown.

4. Effect of KLF15 on allicin-induced UCP1 expression in white adipocytes

To evaluate the potential relationship between KLF15 and UCP1 in allicin-treated white adipocytes, whether KLF15 mediates the expression of UCP1 protein was investigated. Figure 16 shows that the expression of KLF15 was altered by allicin treatment, and it is well-known that UCP-1 and KLF-15 regulate adipogenesis-related genes, adipocyte lipid metabolism, systemic energy balance, and brown adipocyte differentiation [43]. Figure 17 shows that endogenous KLF15 protein expression in 3T3-L1 cells was markedly reduced by RNA silencing. Moreover, depletion of KLF15 protein expression inhibited UCP1 protein expression. Collectively, these data suggest that the protein expression of KLF15 is essential for regulating the protein expression of UCP1.

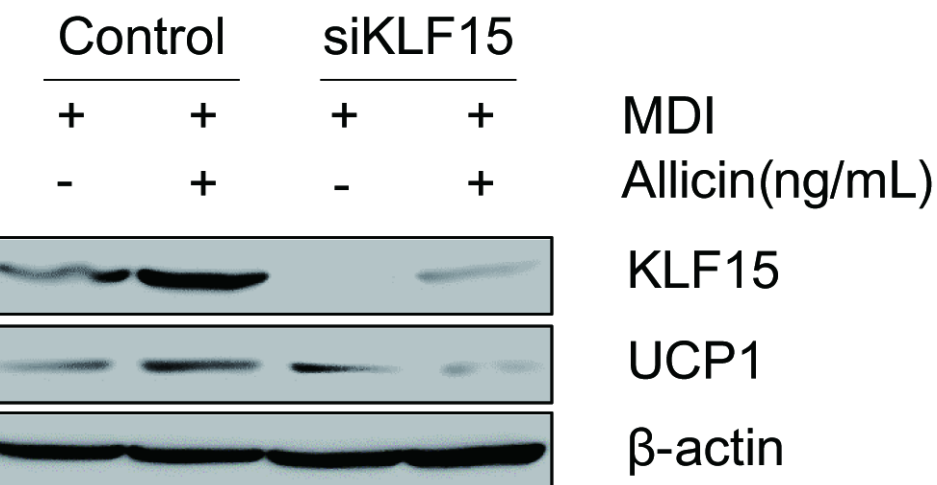


Figure 17. Effect of KLF15 on allicin-induced UCP1 expression in white adipocytes. Reduction of UCP1 by siRNAs against KLF15 in differentiated 3T3-L1 cells. A typical result from three independent experiments is shown.

5. Effect of allicin on phosphorylation of MAPK in white adipocytes

It is widely accepted that the phosphorylation of MAP kinases (MAPKs) is associated with the differentiation of brown adipocytes via the KLF family [80]. The present data show that the protein expression of KLF15 was influenced by allicin. Therefore, phosphorylation of the p38 MAPK, ERK1/2, and JNK kinase pathways was examined to determine whether the MAPK pathway is involved in allicin-induced white adipocyte browning. Figure 18 shows that allicin clearly up-regulated the phosphorylation of ERK1/2, whereas the activation of p38 and JNK was not affected by allicin treatment in differentiated 3T3-L1 cells.

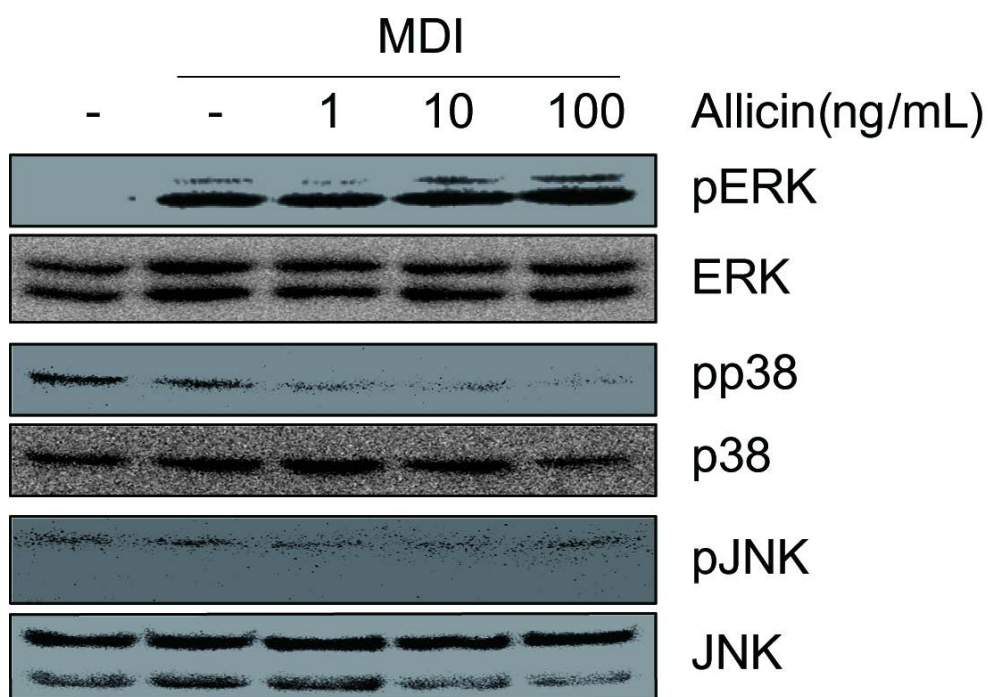
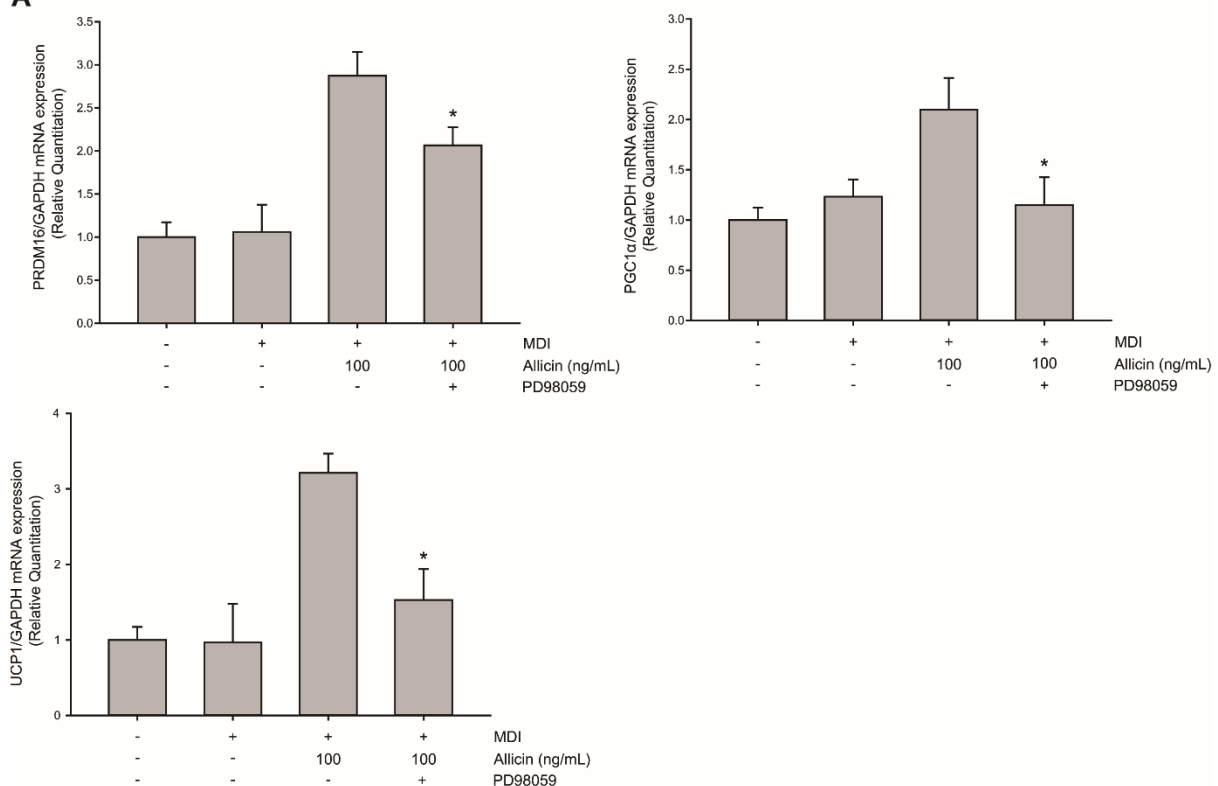
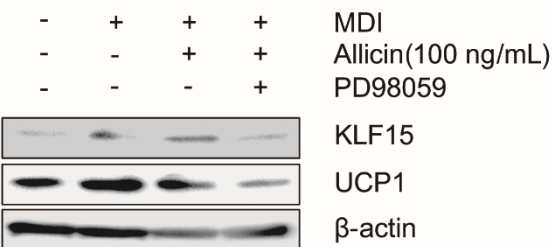
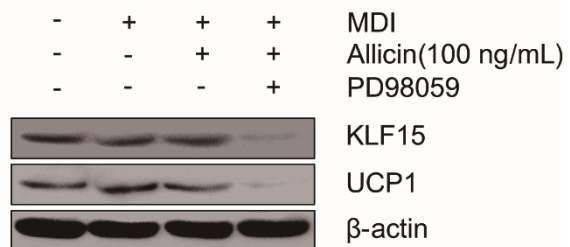


Figure 18. Effect of allicin on activation of MAPK in white adipocytes. 3T3-L1 preadipocytes were cultured in differentiation medium containing 1, 10, and 100 ng/mL of allicin for 2 h. Whole cell lysates were analyzed by western blotting using antibodies specific to phospho-ERK, ERK, phospho-p38, p38, phospho-JNK, and JNK. A typical result derived from three independent experiments is shown.

6. Effect of ERK signaling on allicin-induced browning of white adipocytes

To confirm whether the ERK pathway contributes to allicin-mediated white adipocytes browning, 3T3-1 cells were treated with the MEK inhibitor PD98059 before allicin exposure to examine the mRNA expression of PRDM16, PGC1 α , and UCP1. The results demonstrated that allicin-induced mRNA expression of PRDM16, PGC1 α , and UCP1 was significantly down-regulated by pretreatment with PD98059 (Fig. 19A). Additionally, allicin-induced protein expression of KLF15 and UCP1 was inhibited by PD98059 (Fig. 19B). Similarly, KLF15 and UCP1 expression was inhibited by the MEK inhibitor in iWAT SVCs (Fig. 19B). MitoTracker analysis revealed that allicin-induced mitochondria mass was decreased by pretreatment with PD98059 (Fig. 19C). Taken together, these results suggest that ERK1/2 plays a key role in allicin-mediated white adipocyte browning by regulating the protein expression of pro-brown factors including KLF15.

A**B****3T3-L1****iWAT SVC**

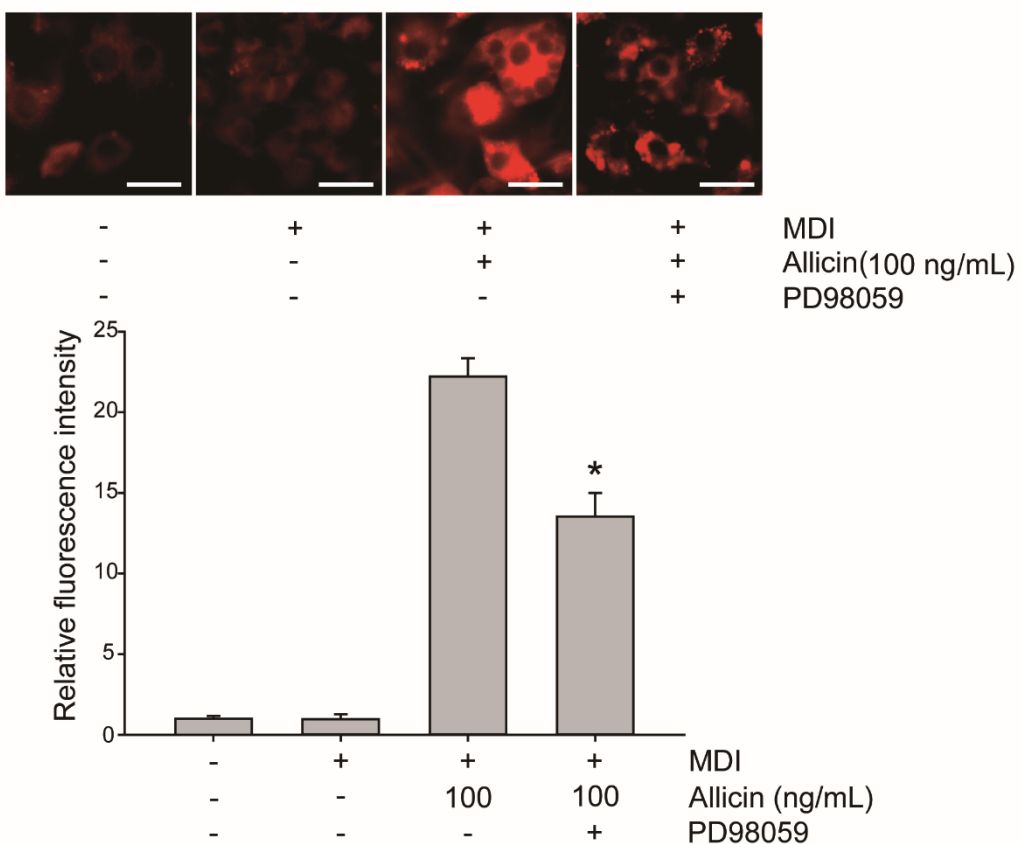
C

Figure 19. Effect of ERK on allicin-induced browning of white adipocytes. 3T3-L1 preadipocytes were pre-incubated with PD98059 (50 μ M) or vehicle for 1 h prior to treatment with allicin for 7 days. (A) Relative mRNA expression of brown adipocyte-specific genes (PRDM16, UCP1, and PGC1 α) in differentiated 3T3-L1 cells. (B) The protein expression of KLF15 and UCP1 in differentiated 3T3-L1 and iWAT SVCs was analyzed by western blotting. A typical result obtained from three independent experiments is shown. (C) Differentiated 3T3-L1 cells were stained with MitoTracker Red. Mitochondrial morphology was analyzed by confocal microscopy. Scale bar, 10 mm. The bar graph represents the percentage of cell populations with fragmented mitochondria. Data are expressed as the means \pm S.E.M. of three independent experiments. *P < 0.05, significantly different from MDI-treated cells.

7. Effect of allicin on association between KLF15 and UCP1 promoter region

A strong interaction has been reported between the KLF15 and UCP1 promoter region in brown adipocyte differentiation [78]. The mouse UCP1 promoter region contains a putative KLF binding site, the cis-acting Sp1 response element (sp1RE). The Sp1RE sequence contains GC-boxes such as CGCCC or GCGGG. Additionally, the present data demonstrated that the protein expression patterns of both KLF15 and UCP1 were up-regulated by allicin treatment and essential for promoting the protein expression of UCP1. However, the relationship between KLF15 and UCP1 in white adipocytes remained unclear. To identify the potential binding sites of the UCP1 promoter to KLF15, a fragment of the UCP1 promoter region (-522 to -122) was analyzed in a chromatin immunoprecipitation (ChIP) assay. As shown in Figure 20A, the GC-box, the potential binding site of KLF, was detected in the UCP1 promoter between position -522 and -122. Chromatin prepared from white adipocytes was cross-linked, sonicated, and precipitated with antibody to KLF15 or IgG followed by reversal of cross-linking and PCR of genomic fragments corresponding to the UCP1 promoters. The ChIP assay data revealed an allicin-induced association of endogenous KLF15 with the fragment of UCP1 promoter containing Sp1RE in differentiated 3T3-L1 cells (Fig. 20B). The regulatory role of ERK1/2 in the protein expression of UCP1 was supported by the suppression of allicin-induced association between KLF15 and the UCP1 promoter region following inhibition of ERK1/2 activity (Fig. 20C). Thus, our data indicate that the association between KLF15 protein and Sp1ER region in the UCP1 promoter was up-regulated by allicin and that allicin-induced activation of ERK1/2 regulated the binding of KLF15 to the UCP1 promoter region.

A

-522 ATCCTCATCCCCACCCCATCCAGTCACCCAAATCTGAAGGTGACATTGAAAAGGAATGTAAAGAAAGG
GACATTCAAGATTGAAAGGAGAAGAACAGTAGCCAAGTAGATGCATGGGAAGGGGGCCCGGGACTGGGA
CGTTCATCCTACAGCTATTCTAGCTGTGGAACCTTCAGCAAAATCTGGAGGAGATCAGATCGCGCTTATTC
AAGGGAACCAGCCCCCTGCT**CTGCGCC**TGGTCCAAGGCTGTTGAAGAGTGACAAAAGGCACCACGCTGCG
Sp1RE
GGGACGCCGGGTGAAGCCCTCTGTGTCTGGGCATAATCAGGAACGGTGCCTGGAGGCTTGCGCACCCA-122

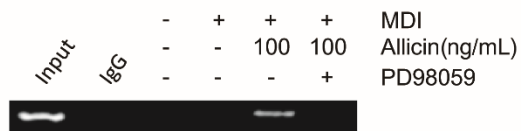
B**C**

Figure 20. Effect of allicin on the association between KLF15 and UCP1 promoter region (A)

Deleted constructs of the mouse UCP1 promoter in the ChIP assay. (B) ChIP assay was performed with or without antibody against KLF15. (C) 3T3-L1 preadipocytes were pre-incubated with PD98059 (50 μ M) or vehicle for 1 h prior to treatment with allicin for 7 days. ChIP assay was performed with or without antibody against KLF15. A typical result from three independent experiments is shown.

8. Effect of allicin on body weight in mice

To investigate the browning effect of allicin on iWAT in vivo, 6-week-old mice were treated with high fat diet (HFD) alone or HFD and oral administration of allicin (1 mg/kg) for 8 weeks. Although significant differences in food intake were not detected (Fig. 21A), the body weight gain in the allicin-administrated group was significantly lower than in the HFD alone group (Fig. 21B). Moreover, allicin-treated mice exhibited decreased iWAT mass (Fig. 21C) and a markedly reduced iWAT index (Fig. 21D). Taken together, these results suggest that oral consumption of allicin reduces body weight and iWAT mass.

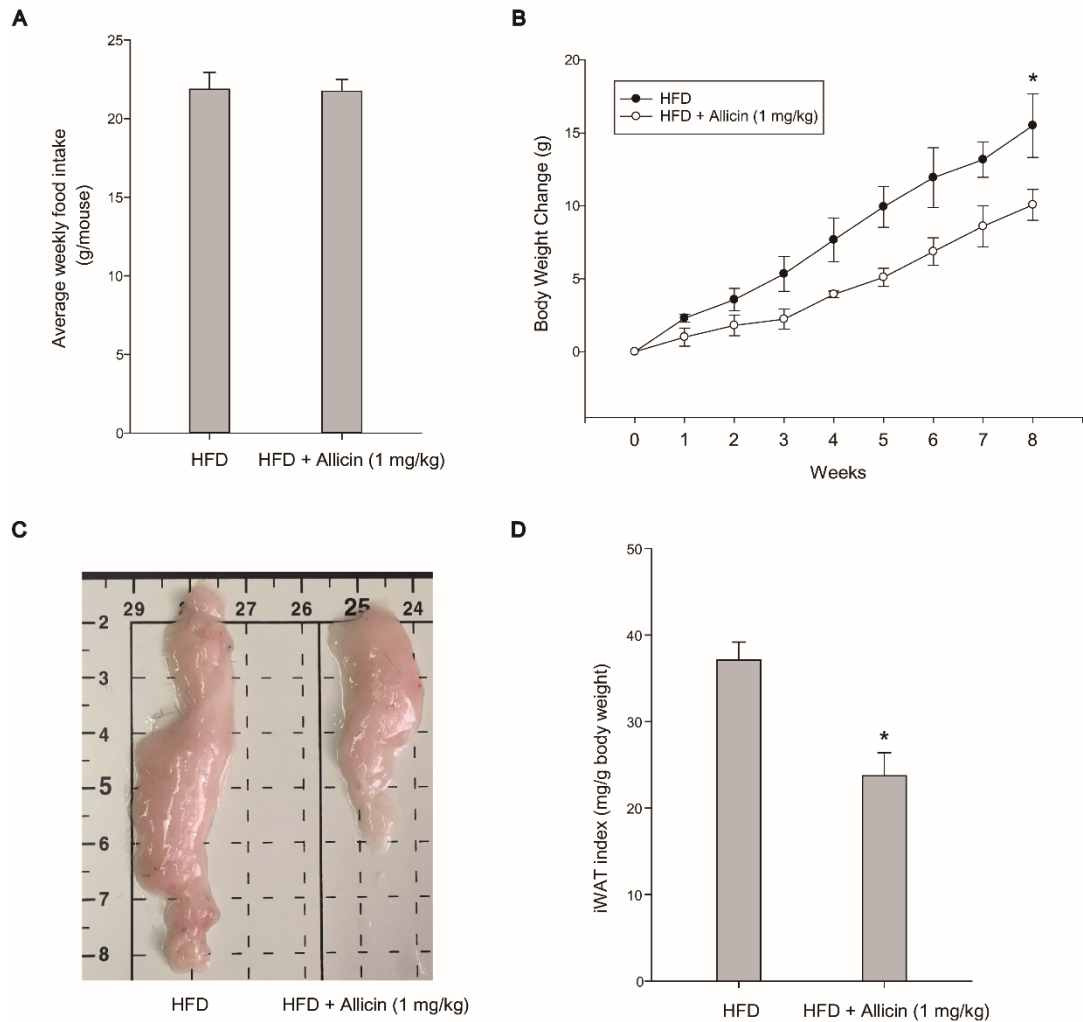
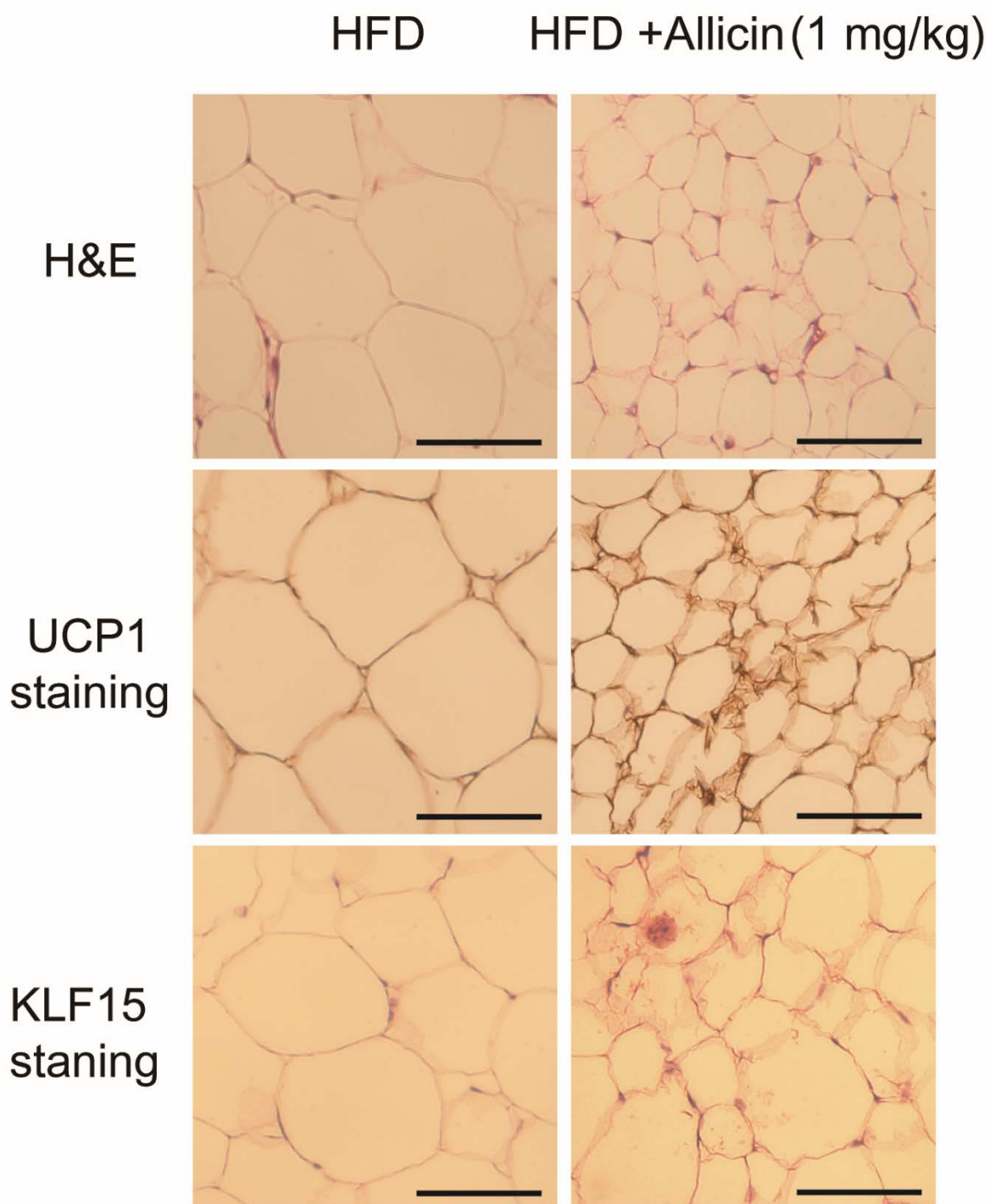


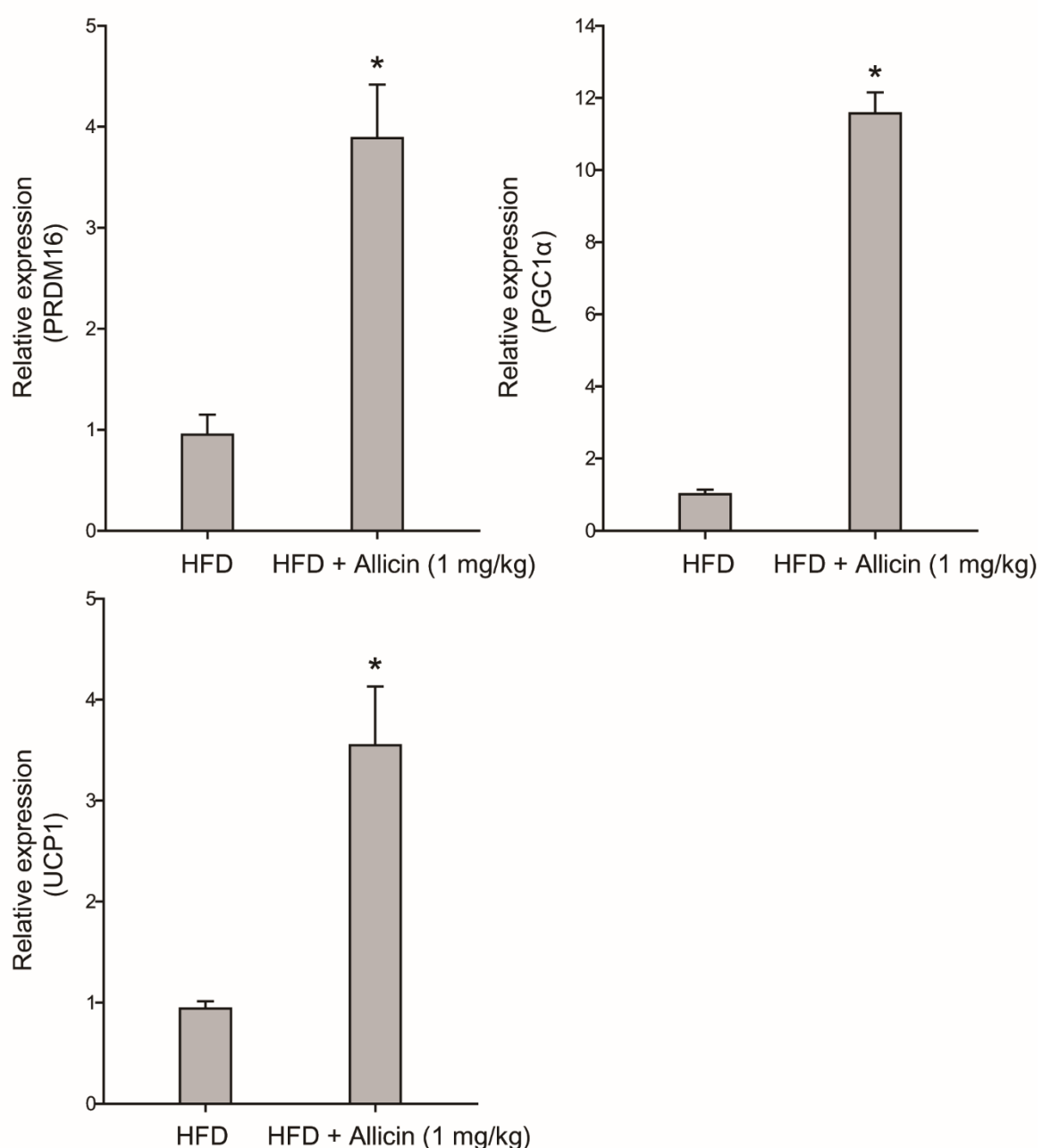
Figure 21. Effect of allicin on body weight in mice. (A) Weekly food intake was measured in the HFD alone ($n = 5$) and allicin-treated ($n = 5$) groups. (B) Body weight changes were compared between the control and allicin-treated groups for 8 weeks. (C) Inguinal WAT fat pads were compared between the control and allicin-treated mice groups. (D) iWAT index was compared between the control and allicin-treated groups. * $P < 0.05$, significantly different from HFD alone group.

9. Effect of allicin on adipocyte browning of iWAT in mice

As shown in Figure 22A, H&E staining revealed that the adipocyte size in the allicin-treated group was much smaller than that in the control group. Additionally, iWAT in the allicin-treated group showed multilocular adipocytes, which is a characteristic of BAT (Fig. 22A). Additional support for these data was derived from immunohistochemical staining of UCP1 and KLF15, which showed that the staining intensity of the target proteins was increased in allicin-treated mice (Fig. 22A). Furthermore, allicin supplementation resulted in increased mRNA expression of PRDM16, PGC1 α , and UCP1 (Fig. 22B) in mouse iWAT. Increased expression of KLF15, UCP1, phospho-ERK, and ERK in the allicin-treated group was also observed (Fig. 22C). The interaction between KLF15 and the UCP1 promoter region was promoted in the allicin-treated group (Fig. 24D). Taken together, these results suggest that allicin induces white adipocyte browning in mouse iWAT. Thus, allicin induced browning of white adipocytes may contribute to the anti-obesity effect of allicin in mice.

A



B

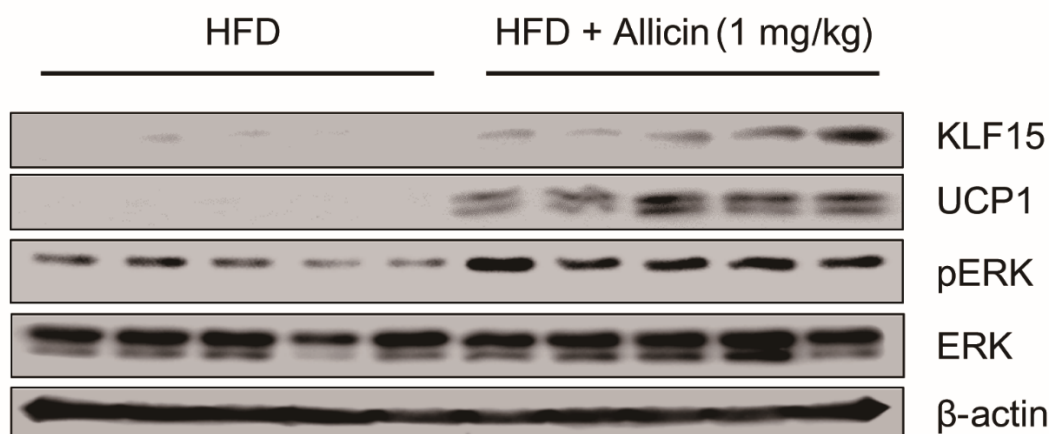
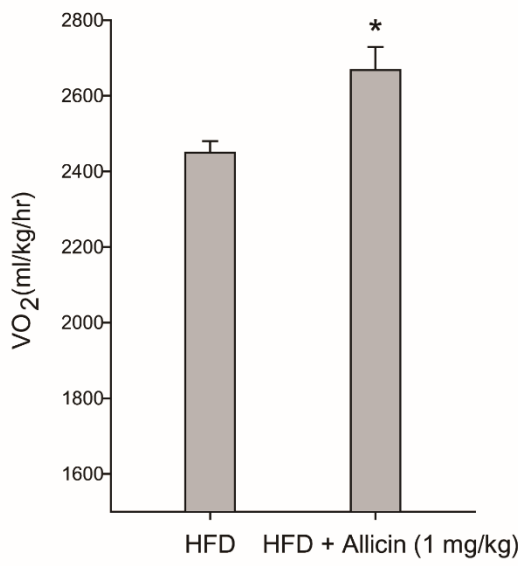
C**D**

Figure 22. Effect of allicin on adipocyte browning of iWAT in mice. (A) Representative images of H&E and UCP1 IHC staining in sections of iWAT of HFD alone and allicin-treated group. All images were obtained at $\times 400$ magnification. (B) Relative mRNA expression of brown adipocyte selective genes (PRDM16, UCP1, and PGC1 α) in iWAT. (C) Whole cell lysates were analyzed by western blotting using antibodies specific to KLF15, UCP1, phospho-ERK, and ERK in iWAT. (D) ChIP assay was performed with or without antibody against KLF15 in iWAT. A typical result from three independent experiments is shown. * $P < 0.05$, significantly different from HFD alone group.

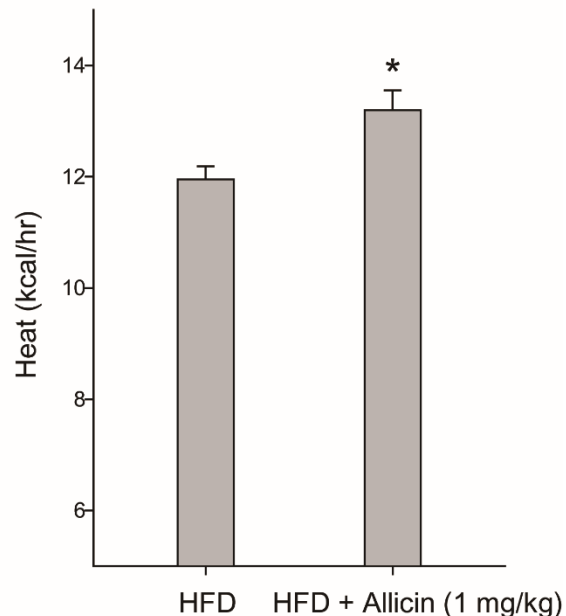
10. Effect of allicin on lipid oxidation and energy expenditure in mice

To investigate the factors contributing to reduced body weight gain and iWAT mass following allicin supplementation, oxygen (O_2) consumption and the RER of mice were assessed by using metabolic cages. RER (CO_2 production/ O_2 consumption) is generally used to indirectly determine the relative contribution of lipids and carbohydrates to ATP production. Lower RER values suggest higher lipid oxidation. In the present study, allicin treatment promoted O_2 consumption (VO_2) in allicin-treated mice (Fig. 23A). Furthermore, the average heat production of mice was increased by oral supplementation with allicin (Fig. 23B). Time-course RER data showed that the RER value began to decline 12 h after allicin administration in allicin-treated mice, indicating greater utilization of lipids by these mice (Fig. 23C).

A



B



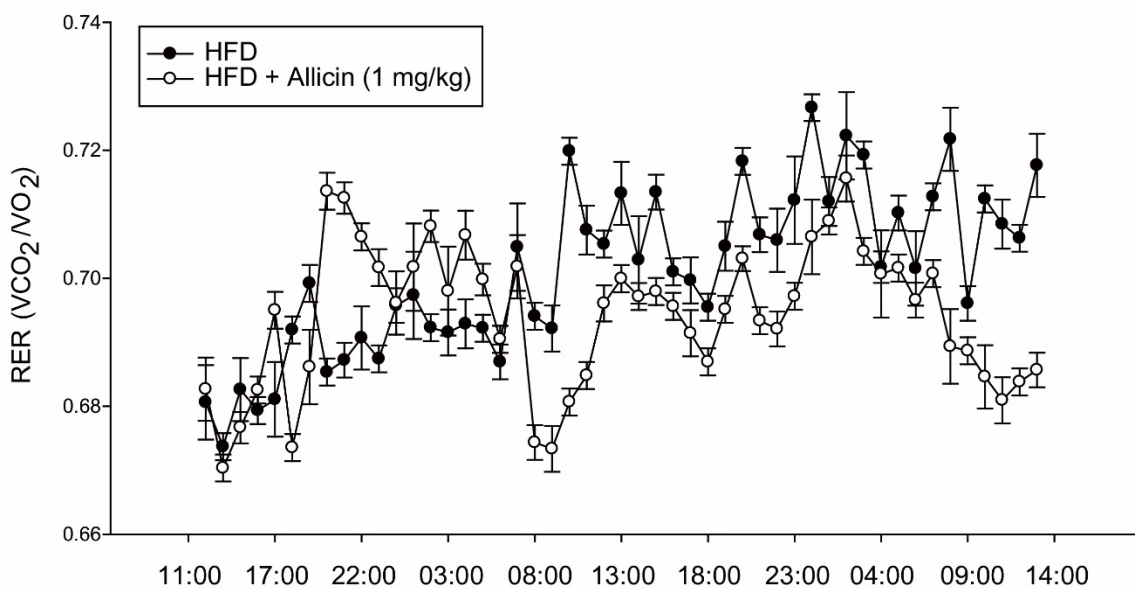
C

Figure 23. Effect of allicin on lipid oxidation and energy expenditure in mice. (A) O_2 consumption of control and allicin-treated mice was recorded during a 48-h period. (B) Average heat production in control and resveratrol-treated mice during a 48-h period. (C) RER of control and resveratrol-treated mice during a 48-h period. * $P < 0.05$, significantly different from HFD alone group.

11. Effect of allicin on lipid metabolism in mice

Analysis of the serum lipid profile in mice was performed to further investigate the effect of allicin on lipid metabolism. Although glucose levels in the mouse serum were not affected by allicin supplementation (Fig. 24A), total cholesterol and triglyceride concentrations were reduced in the allicin-supplemented group compared to in HFD alone group (Fig. 24B). Collectively, these results suggest that oral supplementation of allicin in mice reduced the body weight and lipid accumulation by increasing the contribution of lipids to energy expenditure.

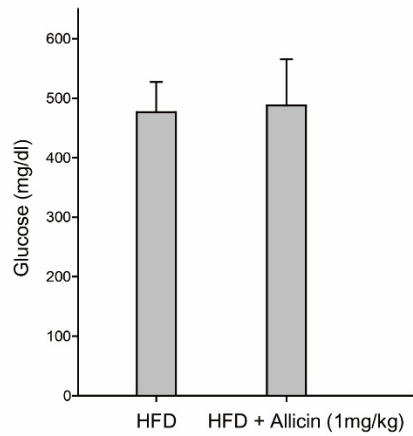
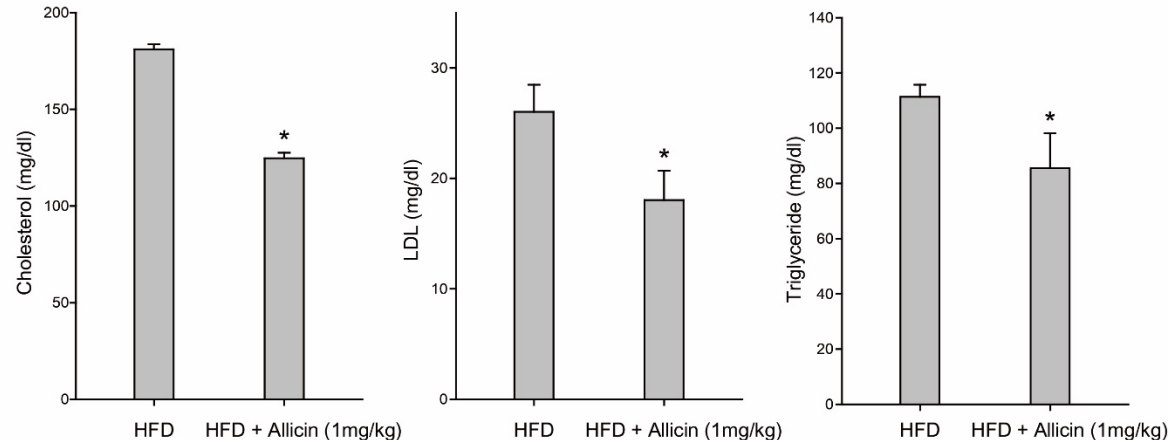
A**B**

Figure 24. Effect of allicin on lipid metabolism in mice. (A) Fasting serum glucose concentrations in control and resveratrol-treated mice. (B) Fasting serum cholesterol, LDL, and triglycerides in control and resveratrol-treated mice. * $P < 0.05$, significantly different from HFD alone group.

IV. DISCUSSION

Obesity is beyond simply being overweight and is no longer considered a personal issue but rather recognized as a chronic disease [81, 82]. Moreover, obesity is closely linked to several metabolic diseases such as insulin resistance and type 2 diabetes mellitus [83, 84] associated with energy imbalance and lipid accumulation [5]. Thus, increasing energy expenditure is beneficial for restoring the energy balance. One method of increasing energy expenditure is to promote the proliferation of brown adipocytes or convert white adipocytes into brown-like adipocytes using pharmacological and nutrition factors [85]. In the present study, the effects of allicin on the formation of brown-like adipocytes and regulatory mechanism underlying this process were investigated. The data show that allicin promotes the browning of differentiated white adipocytes and iWAT by inducing the expression of brown adipocyte-specific genes through KLF15 and ERK1/2. It has been reported that complex hormonal stimulation and numerous environment factors promote WAT browning [86]. Particularly, β -adrenergic agonists convert white adipocytes to brown-like adipocytes [87]. The allyl-containing-sulfides in garlic, including allicin, significantly increase plasma epinephrine and norepinephrine levels in rat [72]. Though it remains unclear whether the adrenergic receptor-mediated signal cascade is fully activated by single administration of allicin, the browning effect of allicin on differentiated white adipocytes may be contributed to the adrenergic receptor-mediated signal pathway. It was recently reported that UCP1 expression is regulated not only by adrenergic receptor-mediated signals but also other membrane receptors, such as estrogen-related receptor-mediated signaling [88]. Thus, to confirm the up-stream regulatory mechanism of allicin-mediate browning effects in differentiated white adipocytes, further studies are needed.

Recent studies have shown that several transcription factors including the KLF family play essential roles in the transcriptional activation of UCP1 and in the final stages of brown adipocyte differentiation [78, 89]. It was also reported that KLF family proteins regulate white adipocyte differentiation. KLF2 inhibits the differentiation of adipocyte progenitor cells by acting as a repressor at the PPAR γ promoter [90]. KLF4 and KLF5 act as activators in the early phase of white adipocyte differentiation [91, 92]. In contrast, KLF15, which is highly expressed in adipocytes and differentiated 3T3-L1 cells, regulates the late stage of differentiation [43]. Moreover, KLF15 plays a role in brown adipocyte differentiation [78]. However, the molecular mechanisms underlying the role of KLF15 in the formation of brown-like adipocytes by allicin are not completely understood. In this study, it was founded that allicin treatment induced the expression of KLF15 in differentiated 3T3-L1 cells and iWAT. Additionally, is the results indicate that KLF15 has a regulatory role in the browning of differentiated 3T3-L1 adipocytes and iWAT by promoting UCP1 expression. This conclusion is based on investigation of the allicin-induced interaction between KLF15 and the UCP1 promoter region, which was up-regulated by allicin treatment in differentiated 3T3-L1 cells and in iWAT. Collectively, these data suggest that allicin-induced expression of UCP1 is promoted by KLF15, which binds to the UCP1 promoter region. However, it cannot be ruled out the possibility that allicin alters the activity of other transcriptional activators, including Zfp516, to regulate UCP1 expression, although the types of stimulants varied. A recent study showed that Zfp516 binds to the UCP1 promoter to promote browning of white fat [93].

MAPKs play a central role in adipocyte proliferation and differentiation. Additionally, MAPKs are activated by numerous stimuli and connect cells via surface receptors to transcription factors in the nucleus [94]. It was reported that MAPK pathways are involved in the adipogenesis of white adipocytes [95]. Moreover, MAPK pathways are differentially involved in the cellular signaling of brown adipocytes, activated by various stimuli [96]. In this

study, the effects of allicin on the ERK1/2, p38 MAPK, and JNK pathways in differentiated 3T3-L1 cells were investigated. The present data show that the phosphorylation of ERK1/2 was increased by allicin treatment, whereas the phosphorylation of p38 MAPK and JNK was slightly decreased by allicin. Allicin-induced phosphorylation of ERK1/2 in iWAT was also found. Because it has been reported that ERK1/2 signaling promotes adipogenesis in brown adipocytes by enhancing PPAR γ [97], which is involved in the browning of differentiated 3T3-L1 cells, allicin-mediated browning of differentiated white adipocytes may be regulated by ERK1/2 through KLF15. To investigate the regulatory effect of ERK1/2 on white adipocyte browning, the mitogen-activated kinase kinase (MEK) inhibitor PD98059 was used. Because MEK1/2 are the only known activators of ERK1/2, PD98059 specifically inhibits the activation of ERK1/2. The protein expression of KLF15 and UCP1 in allicin-treated adipocytes was significantly inhibited by the inhibitor. Additionally, the allicin-induced density of mitochondria was decreased by the inhibitor in differentiated 3T3-L1 cells. Moreover, PD98059 attenuated the allicin-induced interaction between KLF15 and the UCP1 promoter region. Collectively, these data suggest that allicin-induced activation of ERK1/2 regulates the browning of white adipocytes through KLF15.

Because obesity is a complex and chronic disease, it is difficult to investigate the exact mechanisms involved in the long-term process of obesity in humans. To overcome this difficulty, surrogate models including murine genetic loss-of-function mutation, transgenic gain-of-function mutation, and polygenic models and different environmental exposure models are available [98]. In this study, a diet-induced obesity mouse model was used to evaluate the interplay between a high-fat western diet and the effects of allicin on obesity. As a result, allicin induced brown-like adipogenesis in mice iWAT, suggesting that allicin protects mice against high-fat diet-induced obesity. It has been reported that up-regulated brown-like adipocyte formation increases oxygen consumption and lipid oxidation [99, 100]. The present data

indicate that allicin treatment increased oxygen consumption (VO_2) in mice as well as decreased iWAT size and body weight. Consistent with this observation, the expression of genes related to the browning of white adipocytes and heat production were increased in allicin-treated mice. To further determine the mechanism of action of allicin, the time-course of RER levels in mice was investigated. Interestingly, the results showed that RER levels began decreasing at 12 h after allicin treatment. Because RER is commonly used to measure the relative contribution of lipids and carbohydrates to total energy production, a low RER level indicates that lipids were catabolized predominantly, suggesting that allicin promotes predominant catabolism of lipids. Moreover, the reduced iWAT size in allicin-supplemented mice may be attributed to increased lipolysis, subsequent fat oxidation, and increased heat production. However, it remains unclear whether allicin has pharmacological effects in normal-fat diet (NFD) mice. Because excessive lipid accumulation changes normal adipocytes into unhealthy adipocytes, the allicin-induced signal cascade may differ in NFD mice. Thus, while other browning reagents did significantly affect NFD mice [101, 102], further studies are needed in NFD mice to clarify the effect of allicin on mouse iWAT. The simplest interpretation of the present data is that the browning-promoting activity of allicin on iWAT in HFD mice is attributed to its unique pharmacological and health benefits.

Although high reactivity of allicin has been reported, it remains controversial whether allicin is an active compound in garlic. It was previously reported that allicin rapidly transforms into secondary products in the circulation after intravenous injection [58]. Accordingly, allicin was not detected until 3 min of incubation with the blood cell fraction *in vitro* [103]. However, numerous studies have demonstrated the bioavailability and stability of allicin. Research showed that the pH environment of the gastrointestinal tract did not affect the bioavailability of allicin during digestion. Additionally, allicin can penetrate the internal volume of vesicles or cytoplasm of red blood cells without lipid bilayer damage [60, 104]. These findings suggest

that allicin is not degraded rapidly but penetrates cells very rapidly and exerts its biological effect. Within support of this, the present data demonstrated that an allicin-induced reduction in RER was detected 12 h after allicin treatment in mice. Moreover, there are some limitations to using indicators of allicin bioavailability. Because allyl mercaptan, the metabolite of allicin, is also rapidly metabolized, it is difficult to measure the concentration of allyl mercaptan [56]. The detection of breath acetone and allyl methyl sulfide, another metabolite of allicin, is less reliable because of limitations associated with the detector [105]. Thus, further animal and clinical studies are necessary to verify the potential therapeutic use of allicin.

In conclusion, the present study demonstrated that allicin promotes the expression of UCP1 via ERK1/2 activation and KFL15 expression. The data also suggest that allicin induces the formation of brown-like adipocytes in differentiated 3T3-L1 cells and mouse iWAT by increasing the expression of brown adipocyte-specific genes and results in up-regulation of lipid oxidation and energy expenditure. Thus, allicin represents a potential agent for preventing obesity and other metabolic disease, including type 2 diabetes mellitus. Additionally, although the exact role of KFL15 in the mechanism of brown-like adipocyte formation had not been investigated, the present study suggests that KLF15 is a novel therapeutic target for obesity.

V. REFERENCES

1. González-Muniesa, P., et al., *Obesity*. Nature Reviews Disease Primers, 2017. **3**: p. 17034.
2. Organization, W.H., *Obesity and overweight*. <http://www.who.int/mediacentre/factsheets/fs311/en/index.html>, 2013.
3. Sellayah, D., F.R. Cagampang, and R.D. Cox, *On the evolutionary origins of obesity: a new hypothesis*. Endocrinology, 2014. **155**(5): p. 1573-1588.
4. Bhupathiraju, S.N. and F.B. Hu, *Epidemiology of obesity and diabetes and their cardiovascular complications*. Circulation Research, 2016. **118**(11): p. 1723-1735.
5. Hill, J.O., H.R. Wyatt, and J.C. Peters, *Energy balance and obesity*. Circulation, 2012. **126**(1): p. 126-132.
6. Santhanam, P., et al., *Adiposity-related cancer and functional imaging of brown adipose tissue*. Endocrine Practice, 2015. **21**(11): p. 1282-1290.
7. Guertin, D., *Adipocytes*.
8. Kusminski, C.M., P.E. Bickel, and P.E. Scherer, *Targeting adipose tissue in the treatment of obesity-associated diabetes*. Nature Reviews Drug Discovery, 2016. **15**(9):

p. 639.

9. Scherer, P.E., *Adipose tissue: from lipid storage compartment to endocrine organ*. Diabetes, 2006. **55**(6): p. 1537-1545.
10. Rosen, E. and B. Spiegelman, *What we talk about when we talk about fat*. Cell, 2014. **156**(1-2): p. 20.
11. Rutkowski, J.M., J.H. Stern, and P.E. Scherer, *The cell biology of fat expansion*. Journal of Cell Biology, 2015. **208**(5): p. 501-512.
12. Frayn, K., et al., *Integrative physiology of human adipose tissue*. International Journal of Obesity, 2003. **27**(8): p. 875.
13. Spalding, K.L., et al., *Dynamics of fat cell turnover in humans*. Nature, 2008. **453**(7196): p. 783.
14. Sun, K., C. Kusminski, and P. Scherer, *Adipose tissue remodeling and obesity*. The Journal of Clinical Investigation, 2011. **121**(6): p. 2094.
15. Fu, S., S.M. Watkins, and G.S. Hotamisligil, *The Role of Endoplasmic Reticulum in Hepatic Lipid Homeostasis and Stress Signaling*. Cell Metabolism, 2012. **15**(5): p. 623-634.
16. Urano, F., et al., *Coupling of stress in the ER to activation of JNK protein kinases by transmembrane protein kinase IRE1*. Science, 2000. **287**(5453): p. 664-666.

17. Deng, J., et al., *Translational repression mediates activation of nuclear factor kappa B by phosphorylated translation initiation factor 2*. Molecular and Cellular Biology, 2004. **24**(23): p. 10161-10168.
18. Zhang, K., et al., *Endoplasmic reticulum stress activates cleavage of CREBH to induce a systemic inflammatory response*. Cell, 2006. **124**(3): p. 587.
19. Cullinan, S.B. and J.A. Diehl, *Coordination of ER and oxidative stress signaling: the PERK/Nrf2 signaling pathway*. The International Journal of Biochemistry & Cell Biology, 2006. **38**(3): p. 317-332.
20. Lenaz, G., et al., *Role of mitochondria in oxidative stress and aging*. Annals of the New York Academy of Sciences, 2002. **959**(1): p. 199-213.
21. Hotamisligil, G.S., *Inflammation and metabolic disorders*. Nature, 2006. **444**(7121): p. 860.
22. Shukla, A.P., W.I. Buniak, and L.J. Aronne, *Treatment of obesity in 2015*. Journal of Cardiopulmonary Rehabilitation and Prevention, 2015. **35**(2): p. 81-92.
23. Hirosumi, J., et al., *A central role for JNK in obesity and insulin resistance*. Nature, 2002. **420**(6913): p. 333.
24. Nayak, B.S. and L. Roberts, *Relationship between inflammatory markers, metabolic*

and anthropometric variables in the Caribbean type 2 diabetic patients with and without microvascular complications. Journal of Inflammation, 2006. **3**(1): p. 1-7.

25. Lee, Y.-H. and R.E. Pratley, *The evolving role of inflammation in obesity and the metabolic syndrome.* Current Diabetes Reports, 2005. **5**(1): p. 70-75.
26. Ross, R., *Atherosclerosis—an inflammatory disease.* New England Journal of Medicine, 1999. **340**(2): p. 115-126.
27. Velazquez, A. and C. Apovian, *Pharmacological management of obesity.* Minerva Endocrinologica, 2017.
28. Gadde, K.M., et al., *Effects of low-dose, controlled-release, phentermine plus topiramate combination on weight and associated comorbidities in overweight and obese adults (CONQUER): a randomised, placebo-controlled, phase 3 trial.* The Lancet, 2011. **377**(9774): p. 1341-1352.
29. Courcoulas, A., et al., *Weight change and health outcomes at 3 years after bariatric surgery among individuals with severe obesity.* JAMA, 2013. **310**(22): p. 2416.
30. Inge, T.H., et al., *Weight loss and health status 3 years after bariatric surgery in adolescents.* New England Journal of Medicine, 2016. **374**(2): p. 113-123.
31. Ricquier, D., *UCP1, the mitochondrial uncoupling protein of brown adipocyte: a personal contribution and a historical perspective.* Biochimie, 2017. **134**: p. 3-8.

32. Rousset, S., et al., *The biology of mitochondrial uncoupling proteins*. Diabetes, 2004. **53**(suppl 1): p. S130-S135.
33. Cannon, B. and J. Nedergaard, *The biochemistry of an inefficient tissue: brown adipose tissue*. Essays in Biochemistry, 1985. **20**: p. 110.
34. Nicholls, D.G. and R.M. Locke, *Thermogenic mechanisms in brown fat*. Physiological Reviews, 1984. **64**(1): p. 1-64.
35. Brondani, L., et al., *The role of the uncoupling protein 1 (UCP1) on the development of obesity and type 2 diabetes mellitus*. Arquivos Brasileiros de Endocrinologia e Metabologia, 2012. **56**(4): p. 215.
36. Kozak, L. and R. Anunciado-Koza, *UCP1: its involvement and utility in obesity*. International Journal of Obesity, 2009. **32**(S7): p. S32.
37. Harms, M. and P. Seale, *Brown and beige fat: development, function and therapeutic potential*. Nature Medicine, 2013. **19**(10): p. 1252.
38. Cohen, P. and B.M. Spiegelman, *Brown and beige fat: molecular parts of a thermogenic machine*. Diabetes, 2015. **64**(7): p. 2346-2351.
39. Ye, L., et al., *Fat cells directly sense temperature to activate thermogenesis*. Proceedings of the National Academy of Sciences USA, 2013. **110**(30): p. 12480-12485.

40. Wu, J., P. Cohen, and B.M. Spiegelman, *Adaptive thermogenesis in adipocytes: is beige the new brown?* Genes & Development, 2013. **27**(3): p. 234-250.
41. Kajimura, S., B. Spiegelman, and P. Seale, *Brown and beige fat: physiological roles beyond heat generation.* Cell Metabolism, 2015. **22**(4): p. 546.
42. Virtanen, K.A., et al., *Beige adipocytes are a distinct type of thermogenic fat cell in mouse and human.* Cell, 2012. **150**: p. 366-376.
43. Matoba, K., et al., *Adipose KLF15 controls lipid handling to adapt to nutrient availability.* Cell Reports, 2017. **21**(11): p. 3129-3140.
44. Quarta, C., R. Schneider, and M.H. Tschöp, *Epigenetic ON/OFF switches for obesity.* Cell, 2016. **164**(3): p. 341-342.
45. Kajimura, S., *Engineering fat cell fate to fight obesity and metabolic diseases.* The Keio Journal of Medicine, 2015. **64**(4): p. 65-65.
46. Yoneshiro, T., et al., *Recruited brown adipose tissue as an antiobesity agent in humans.* The Journal of Clinical Investigation, 2013. **123**(8): p. 3404.
47. Peng, X., et al., *Unlock the thermogenic potential of adipose tissue: pharmacological modulation and implications for treatment of diabetes and obesity.* Frontiers in Endocrinology, 2015. **6**: p. 174.

48. Ishibashi, J. and P. Seale, *Beige can be slimming*. Science, 2010. **328**(5982): p. 1113-1114.
49. Lawson, L.D., *Garlic: a review of its medicinal effects and indicated active compounds*. Phytomedicines of Europe: Chemistry and Biological Activity. Washington, DC: American Chemical Society, 1998: p. 176-209.
50. Bayan, L., P.H. Koulivand, and A. Gorji, *Garlic: a review of potential therapeutic effects*. Avicenna Journal of Phytomedicine, 2014. **4**(1): p. 1.
51. Colín-González, A.L., et al., *The antioxidant mechanisms underlying the aged garlic extract-and S-allylcysteine-induced protection*. Oxidative Medicine and Cellular Longevity, 2012. **2012**.
52. Aviello, G., et al., *Garlic: empiricism or science?* Natural Product Communications, 2009. **4**(12): p. 1785-1796.
53. Koseoglu, M., et al., *Effects of acute and subacute garlic supplement administration on serum total antioxidant capacity and lipid parameters in healthy volunteers*. Phytotherapy Research: An International Journal Devoted to Pharmacological and Toxicological Evaluation of Natural Product Derivatives, 2010. **24**(3): p. 374-378.
54. Stevinson, C., M.H. Pittler, and E. Ernst, *Garlic for treating hypercholesterolemia: a meta-analysis of randomized clinical trials*. Annals of Internal Medicine, 2000. **133**(6):

p. 420-429.

55. Lee, M.-S., et al., *Reduction of body weight by dietary garlic is associated with an increase in uncoupling protein mRNA expression and activation of AMP-activated protein kinase in diet-induced obese mice–3*. The Journal of Nutrition, 2011. **141**(11): p. 1947-1953.
56. Marchese, A., et al., *Antifungal and antibacterial activities of allicin: A review*. Trends in Food Science & Technology, 2016. **52**: p. 49-56.
57. Ankri, S. and D. Mirelman, *Antimicrobial properties of allicin from garlic*. Microbes and Infection, 1999. **1**(2): p. 125-129.
58. Lawson, L.D. and C.D. Gardner, *Composition, stability, and bioavailability of garlic products used in a clinical trial*. Journal of Agricultural and Food Chemistry, 2005. **53**(16): p. 6254-6261.
59. Amagase, H., *Clarifying the real bioactive constituents of garlic*. The Journal of Nutrition, 2006. **136**(3): p. 716S-725S.
60. Omar, S. and N. Al-Wabel, *Organosulfur compounds and possible mechanism of garlic in cancer*. Saudi Pharmaceutical Journal, 2010. **18**(1): p. 51-58.
61. Yang, J.Y., et al., *Molecular mechanisms of apoptosis induced by ajoene in 3T3-L1 adipocytes*. Obesity, 2006. **14**(3): p. 388-397.

62. Keophiphath, M., et al., *1, 2-vinyldithiin from garlic inhibits differentiation and inflammation of human preadipocytes*. The Journal of Nutrition, 2009. **139**(11): p. 2055-2060.
63. Horev-Azaria, L., et al., *Allicin up-regulates cellular glutathione level in vascular endothelial cells*. European Journal of Nutrition, 2009. **48**(2): p. 67-74.
64. Liu, C., et al., *Allicin protects against cardiac hypertrophy and fibrosis via attenuating reactive oxygen species-dependent signaling pathways*. The Journal of Nutritional Biochemistry, 2010. **21**(12): p. 1238-1250.
65. Higashi, Y., et al., *Endothelial function and oxidative stress in cardiovascular diseases*. Circulation Journal, 2009. **73**(3): p. 411-418.
66. Stewart, Z.A., M.D. Westfall, and J.A. Pietenpol, *Cell-cycle dysregulation and anticancer therapy*. Trends in Pharmacological Sciences, 2003. **24**(3): p. 139-145.
67. McKenzie, S. and N. Kyprianou, *Apoptosis evasion: the role of survival pathways in prostate cancer progression and therapeutic resistance*. Journal of Cellular Biochemistry, 2006. **97**(1): p. 18-32.
68. Trio, P.Z., et al., *Chemopreventive functions and molecular mechanisms of garlic organosulfur compounds*. Food & Function, 2014. **5**(5): p. 833-844.

69. Powolny, A.A. and S.V. Singh, *Multitargeted prevention and therapy of cancer by diallyl trisulfide and related Allium vegetable-derived organosulfur compounds*. Cancer Letters, 2008. **269**(2): p. 305-314.
70. Bruck, R., et al., *Allicin, the active component of garlic, prevents immune-mediated, concanavalin A-induced hepatic injury in mice*. Liver International, 2005. **25**(3): p. 613-621.
71. Dirsch, V.M., et al., *Effect of allicin and ajoene, two compounds of garlic, on inducible nitric oxide synthase*. Atherosclerosis, 1998. **139**(2): p. 333-339.
72. Oi, Y., et al., *Allyl-containing sulfides in garlic increase uncoupling protein content in brown adipose tissue, and noradrenaline and adrenaline secretion in rats*. The Journal of Nutrition, 1999. **129**(2): p. 336-342.
73. Bureau, C., et al., *Expression and function of Kruppel like-factors (KLF) in carcinogenesis*. Current Genomics, 2009. **10**(5): p. 353-360.
74. Kaczynski, J., T. Cook, and R. Urrutia, *Sp1-and Krüppel-like transcription factors*. Genome Biology, 2003. **4**(2): p. 206.
75. Uchida, S., et al., *Transcriptional regulation of the CLC-K1 promoter by myc-associated zinc finger protein and kidney-enriched Krüppel-like factor, a novel zinc finger repressor*. Molecular and Cellular Biology, 2000. **20**(19): p. 7319-7331.

76. Mori, T., et al., *Role of Krüppel-like factor 15 (KLF15) in transcriptional regulation of adipogenesis*. Journal of Biological Chemistry, 2005. **280**(13): p. 12867-12875.
77. Nagare, T., et al., *Overexpression of KLF15 transcription factor in adipocytes of mice results in down-regulation of SCD1 protein expression in adipocytes and consequent enhancement of glucose-induced insulin secretion*. Journal of Biological Chemistry, 2011. **286**(43): p. 37458-37469.
78. Yamamoto, K.-i., et al., *Transcriptional regulation of a brown adipocyte-specific gene, UCP1, by KLF11 and KLF15*. Biochemical and Biophysical Research Communications, 2010. **400**(1): p. 175-180.
79. Takeuchi, Y., et al., *KLF15 enables rapid switching between lipogenesis and gluconeogenesis during fasting*. Cell Reports, 2016. **16**(9): p. 2373-2386.
80. McConnell, B.B. and V.W. Yang, *Mammalian Krüppel-like factors in health and diseases*. Physiological Reviews, 2010. **90**(4): p. 1337-1381.
81. Mello, M.M., *Obesity—personal choice or public health issue?* Nature Reviews Endocrinology, 2007. **4**(1): p. 2.
82. Brownell, K.D., et al., *Personal responsibility and obesity: a constructive approach to a controversial issue*. Health Affairs, 2010. **29**(3): p. 379-387.
83. Tuomilehto, J., et al., *Prevention of type 2 diabetes mellitus by changes in lifestyle*

among subjects with impaired glucose tolerance. The New England Journal of Medicine, 2001. **344**(18): p. 1343-1350.

84. Group, D.P.P.R., *Reduction in the incidence of type 2 diabetes with lifestyle intervention or metformin.* New England Journal of Medicine, 2002. **300**(346): p. 393-403.
85. Eckel, R.H., et al., *Obesity and type 2 diabetes: what can be unified and what needs to be individualized?* The Journal of Clinical Endocrinology & Metabolism, 2011. **96**(6): p. 1654-1663.
86. Bartelt, A. and J. Heeren, *Adipose tissue browning and metabolic health.* Nature Reviews Endocrinology, 2014. **10**(1): p. 24-36.
87. Ohno, H., et al., *PPAR γ agonists induce a white-to-brown fat conversion through stabilization of PRDM16 protein.* Cell Metabolism, 2012. **15**(3): p. 395-404.
88. Brown, E.L., et al., *Estrogen-related receptors mediate the adaptive response of brown adipose tissue to adrenergic stimulation.* iScience, 2018. **2**: p. 221-237.
89. Gesta, S., Y. Tseng, and C. Kahn, *Developmental origin of fat: tracking obesity to its source.* Cell, 2007. **131**(2): p. 242-256.
90. Banerjee, S.S., et al., *The Krüppel-like factor KLF2 inhibits peroxisome proliferator-activated receptor- γ expression and adipogenesis.* Journal of Biological Chemistry, 2003. **278**(4): p. 2581-2584.

91. Oishi, Y., et al., *Krüppel-like transcription factor KLF5 is a key regulator of adipocyte differentiation*. Cell Metabolism, 2005. **1**(1): p. 27.
92. Birsoy, K., Z. Chen, and J. Friedman, *Transcriptional regulation of adipogenesis by KLF4*. Cell Metabolism, 2008. **7**(4): p. 339-347.
93. Dempersmier, J., et al., *Cold-inducible Zfp516 activates UCP1 transcription to promote browning of white fat and development of brown fat*. Molecular Cell, 2015. **57**: p. 235-246.
94. Whitmarsh, A.J., *Regulation of gene transcription by mitogen-activated protein kinase signaling pathways*. Biochimica et Biophysica Acta (BBA)-Molecular Cell Research, 2007. **1773**(8): p. 1285-1298.
95. Bost, F., et al., *The role of MAPKs in adipocyte differentiation and obesity*. Biochimie, 2005. **87**(1): p. 51-56.
96. Bordicchia, M., et al., *Cardiac natriuretic peptides act via p38 MAPK to induce the brown fat thermogenic program in mouse and human adipocytes*. The Journal of Clinical Investigation, 2012. **122**(3): p. 1022.
97. Prusty, D., et al., *Activation of MEK/ERK signaling promotes adipogenesis by enhancing peroxisome proliferator-activated receptor γ (PPAR γ) and C/EBP α gene expression during the differentiation of 3T3-L1 preadipocytes*. Journal of Biological

Chemistry, 2002. **277**(48): p. 46226-46232.

98. Wang, C.-Y. and J.K. Liao, *A mouse model of diet-induced obesity and insulin resistance*, in *mTOR*. 2012, Springer. p. 421-433.
99. Wang, S., et al., *Resveratrol induces brown-like adipocyte formation in white fat through activation of AMP-activated protein kinase (AMPK) α1*. International Journal of Obesity, 2015. **39**(6): p. 967-976.
100. Zhang, Y., et al., *Irisin stimulates browning of white adipocytes through mitogen-activated protein kinase p38 MAP kinase and ERK MAP kinase signaling*. Diabetes, 2014. **63**(2): p. 514-525.
101. Zou, T., et al., *Resveratrol supplementation of high-fat diet-fed pregnant mice promotes brown and beige adipocyte development and prevents obesity in male offspring*. The Journal of Physiology, 2017. **595**(5): p. 1547-1562.
102. Wang, S., et al., *Resveratrol induces brown-like adipocyte formation in white fat through activation of AMP-activated protein kinase (AMPK) α1*. International Journal of Obesity, 2015. **39**(6): p. 967.
103. Rahman, M.S., *Allicin and other functional active components in garlic: health benefits and bioavailability*. International Journal of Food Properties, 2007. **10**(2): p. 245-268.
104. Freeman, F. and Y. Kodera, *Garlic chemistry: stability of S-(2-propenyl)-2-propene-1-*

sulfinothioate (allicin) in blood, solvents, and simulated physiological fluids. Journal of Agricultural and Food Chemistry, 1995. **43**(9): p. 2332-2338.

105. Lawson, L.D. and Z.J. Wang, *Allicin and allicin-derived garlic compounds increase breath acetone through allyl methyl sulfide: use in measuring allicin bioavailability.* Journal of Agricultural and Food Chemistry, 2005. **53**(6): p. 1974-1983.

국문초록

전사인자 KLF15를 통해 이루어지는 Allicin의 유사갈색지방세포 형성 효과 연구

이충기

성균관대학교 대학원

약학과

비만은 지방조직, 특히 백색지방이 지나치게 축적된 상태를 의미한다. 비만은 대부분 약한 염증상태를 동반하기 때문에 비만에 의해 인슐린 저항성, 제2형 당뇨, 암과 같은 대사질환이 유발될 수 있다고 알려져 있다. 비만치료를 위해서 생활습관 개선을 위한 행동요법, 약물요법, 외과적 수술과 같은 방법들이 이루어지고 있지만 부작용과 같은 한계가 있기 때문에 더 안전하고 효과적인 비만 치료제의 개발이 필요하다. 최근 들어 주변 온도의 변화나 체내 호르몬, 효소와 같은 자극을 통해서 백색지방의 갈색지방화가 유도된다는 보고가 증가함에 따라 이러한 유사갈색지방세포의 증가를 통해 비만을 치료하고자 하는 연구가 활발히 진행

되고 있다. 하지만 식품에서 유래된 성분들이 직접적으로 백색지방의 갈색지방화를 유도하는지에 대한 연구는 아직 미비한 실정이다. 따라서 본 연구에서는 비만치료효과를 가지는 새로운 후보 물질을 찾기 위해서 마늘의 가장 주된 성분 중 하나인 Allicin이 백색지방에 미치는 효과를 연구하였다. Allicin이 백색지방의 갈색지방화 효과를 가진다는 가설을 세우고 Allicin이 *in vitro* 상에서 백색지방세포에 어떠한 영향을 미치는지를 연구하였다. 또한 동물모델에서 Allicin이 지방의 대사과정에 미치는 영향과 비만억제 효과를 가지는지에 대해서도 연구 하였다. 그 결과, 분화된 3T3-L1 전구지방세포와 분화 된 서혜부 백색지방조직 (inguinal white adipose tissue, iWAT)의 기질혈관세포 (stromal vascular cell, SVC)에서 갈색지방 특이적으로 발현된다고 알려진 UCP1과 같은 인자들의 mRNA와 단백질 발현이 Allicin에 의해 현저하게 증가하는 것을 확인하였다. 이 결과는 *in vitro*에서 Allicin이 유사갈색지방의 생성을 유도할 수 있다는 것을 의미한다. 뿐만 아니라, Allicin에 의해 전사인자 KLF15 단백질 발현이 증가하고 *UCP1* 유전자의 promoter 부분과 KLF15의 결합 역시 증가하는 것을 확인하였다. 하지만 KLF15의 발현을 억제시킨 분화된 백색지방세포에서는 Allicin에 의한 유사갈색지방 형성유도 효과를 관찰할 수 없었다. 이 결과는 Aliicin의 백색지방의 갈색지방화 기전에서 KLF15가 핵심적인 역할을 한다는 것을 의미한다. 다음으로, Allicin을 경구투여 한 mouse 모델에서 Allicin이 mouse에 미치는 영향을 확인하였다. 그 결과, Allicin에 의해서 mouse의 체중증가가 억제되는 것을 확인하였고, mouse iWAT가 갈색지방의 특징인 다방성 (multilocular) 양상을 나타내는 것과, 지방조직 내에서 KLF15, UCP1 단백질의 발현이 증가되며 mouse 체내 지방의 산화가 증가되는 것을 관찰할 수 있었다. 관찰한 결과들을 종합 해 볼 때, 전사인자 KLF15를 통해서 UCP1 발현을 촉진시키고

백색지방의 유사갈색지방화를 유발하는 Allicin의 효과를 규명할 수 있었다. 동물 모델에서 확인한 Allicin의 비만억제효과는 Allicin의 유사갈색지방 형성효과에 기인한다고 할 수 있다. 따라서 이번 연구를 통해서 Allicin이 효과적인 비만치료제로 개발될 수 있다는 가능성을 제시할 수 있었다. 나아가, 비만으로 인한 과도한 지방조직의 축적은 인슐린 저항성 증가나 제2형 당뇨병과 같은 대사성질환의 위험인자이기 때문에, Allicin이 비만성 대사질환의 새로운 약물요법으로 사용될 수 있는 가능성 역시 제시할 수 있다.